Dynamic regulation of protein homeostasis underlies acquired thermotolerance in *Arabidopsis thaliana*

Mayur Bajaj[1], Annapurna Devi Allu[1*], Basuthkar J Rao[1,2*]

[1]Department of Biology, Indian Institute of Science Education and Research (IISER), Tirupati - 517619, INDIA

[2]Department of Animal Biology, School of Life Sciences, University of Hyderabad, Hyderabad - 500046, INDIA

* Co-corresponding authors – anu.allu@iisertirupati.ac.in; bjrao@uohyd.ac.in

Abstract

Rapid climate change necessitates the development of heat-stress resilient plants. Elevated temperatures perturb cellular protein homeostasis, and its timely restoration is critical for plant survival post-stress. Thermopriming, which involves pre-exposure to sublethal heat stress, has emerged as a promising approach to enhance heat stress tolerance. However, the impact of thermopriming on protein homeostasis remains unclear. This study demonstrates that priming-mediated short-term acquired thermotolerance involves dynamic regulation of protein maintenance (HSPs) and clearance (autophagy) mechanisms. Priming facilitates an increase in HSP abundance through HSFA1 activation. Concurrently, priming induces autophagy through dynamic modulation of autophagy-negative regulators through IRE1's-mRNA degradation activity. Contrarily, unprimed seedlings fail to exhibit such coordinated regulation, resulting in disrupted proteostasis and fail to survive. While the loss of IRE1 had minimal impact on priming-mediated outcomes, HSFA1 proved essential, as its absence led to lethality under heat stress. This underscores the critical role of protein maintenance mechanisms over clearance pathways in ensuring survival. Taken together, our study demonstrates that thermopriming enhances heat stress resilience by temporally coordinating autophagy and chaperone responses to maintain proteostasis.

Keywords

Autophagy, ER stress, Heat Shock Factor A1, Priming, Thermotolerance

Introduction

In nature, plants often encounter multiple abiotic and biotic stresses which affects their cellular homeostasis. High temperature is one such abiotic stressor that is detrimental to plant growth, productivity and even survival. Heat stress reduces protein, starch, and oil content (Fahad et al., 2017) and can cause substantial economic losses in agriculture (Long & Ort, 2010; Schmitt et al., 2022). Studies have reported that for every 2°C rise in temperature, there could be a 50% decline in crop productivity (Lobell et al., 2012). As sessile organisms, plants cannot escape adverse conditions and must instead preemptively activate protective genes to survive. Recent studies identified that pre-exposure to a stress stimulus (referred to as 'priming') can dramatically improve plant stress tolerance.

'Priming' is a memory-based physiological response in which an organism mounts a heightened defense response to subsequent stresses (Conrath, 2011; Conrath et al., 2007; Wilkinson et al., 2019). Several stimuli including mild environmental stress factors, hormones or chemical moieties can serve as priming agents (Nair et al., 2022). Priming-mediated acquired stress tolerance has been previously studied in the model plant system *Arabidopsis thaliana* along with several crop plants (Balmer et al., 2018; Liu et al., 2021; Samantaray et al., 2023; Song et al., 2015; Westman et al., 2019; Ye et al., 2019). Priming can aid in remodeling the transcriptomic, epigenetic, or metabolic programs, increasing the robustness of plant response to subsequent stress (Catoni et al., 2022; Espinas et al., 2016; Gamir et al., 2014; Serrano et al., 2019; Tugizimana et al., 2018). While several studies focused on understanding the epigenetic regulation underlying priming response (Crespo-Salvador et al., 2018; Kotkar & Giri, 2020; Noh et al., 2021; Turgut-Kara et al., 2020), very little is known about the role of post-transcriptional processes such as protein homeostasis, autophagy and mitochondrial dynamics, which are critical for plant survival (Raffeiner et al., 2023; Selinski et al., 2024; Sun et al., 2021).

Heat stress primarily disrupts protein homeostasis by destabilizing thermolabile protein molecules (Richter et al., 2010). In response, plants activate multiple proteostasis pathways - including molecular chaperones, autophagy, and the ubiquitin-proteasome system (UPS) - to restore protein homeostasis and promote stress tolerance. Upon heat stress, misfolded proteins accumulate thereby activating heat shock response (HSR) in cytosol, and unfolded protein response (UPR) in endoplasmic reticulum (Gao et al., 2023). HSR involves accumulation of heat shock proteins (HSPs), which facilitates the refolding and disaggregation of misfolded proteins (Richter et al., 2010; Rosenzweig et al., 2019). *HSFA2* and *HSFA3* are well-established HSR molecules involved in transcriptional upregulation of chaperones under

acclimatizing heat stress conditions (Friedrich et al., 2021). Additionally, proteotoxic stress also activates degradative pathways- UPS and autophagy. Where UPS is involved in clearance of unfolded/misfolded proteins, autophagy contributes by removing damaged organelles and promotes the recycling of dysfunctional proteins/aggregates during heat stress (Raffeiner et al., 2023; Sharma et al., 2024; Su et al., 2020; Zhou et al., 2013). Autophagy is tightly regulated by signaling pathways involving TOR, SnRK, and IRE1. TOR (Target of rapamycin) inhibits autophagy under nutrient-rich conditions by phosphorylating components of the autophagy initiation complex (Suttangkakul et al., 2011), whereas, SnRK (sucrose non-fermenting 1 (SNF1)-related protein kinase) promotes autophagy during energy deprivation by inhibiting TOR (Soto-Burgos & Bassham, 2017). IRE1 (Inositol-requiring 1), an endoplasmic reticulum (ER) membrane protein, gets activated during ER stress (Nawkar et al., 2018; Pastor-Cantizano et al., 2020) and is proposed to positively regulate autophagy via its mRNA degradation activity (Bao et al., 2018). Additionally, HSFA1a has also been identified to induce autophagy under heat and drought stress by upregulating *ATG* genes (Wang et al., 2015; Xie et al., 2022). Autophagy also plays a role in resetting long-term heat-stress memory (Sedaghatmehr et al., 2019) by degrading specific chaperones HSP21 and HSP90.1, through FtsH6- and NBR1-mediated mechanisms, respectively (Sedaghatmehr et al., 2021; Thirumalaikumar et al., 2020). However, how protein homeostasis mechanisms contribute towards priming-mediated responses remains understudied.

In this study, we examined the regulation of protein homeostasis pathways to gain insights into the post-transcriptional regulatory landscape and its role in short-term heat stress memory. Our findings suggest that thermopriming enhances thermotolerance by concurrently activating protein maintenance and protection through the accumulation of chaperones, as well as facilitates protein clearance via autophagy. Conversely, unprimed seedlings fail to activate the protein protective response, leading to disruption of proteostasis and ultimately failing to survive severe heat stress. Overall, our study offers novel insights into priming-induced heat stress tolerance, highlighting the critical role of protein homeostasis in maintaining cellular resilience under thermal stress.

Methods

Plant materials and growth conditions

Arabidopsis thaliana (Col-0-referred to as WT and Ws-0-referred to as Ws-0) seeds were surface sterilized by washing with 80% ethanol for 30 seconds (s) followed by 1% bleach for 3 minutes (min),

117 and 3x washes with sterile double distilled water. Seeds were then sown on ½ Murashige and Skoog
118 media with 1% sucrose and 0.8% agar powder. The seeds were stratified at 4°C for two days before
119 transferring them to growth chambers with 16 hour (h) light and 8h dark, 65% humidity. The five-day-
120 old *Arabidopsis* seedlings were primed by exposing them to 37°C for 90 min, followed by a recovery
121 at 22°C for 90 min, and heat-triggering at 45°C for 45 min. The unprimed seedlings were directly
122 exposed to 45°C for 45 min. For the primed-control condition, seedlings were only subjected to a 37°C
123 treatment for 90 min and were returned to optimal growth conditions. Control seedlings were maintained
124 at optimal growth conditions (22°C, 16h light and 8h dark, 65% humidity) throughout the experiment.
125 Seedlings were harvested at different stress recovery time points for gene expression and protein
126 analysis. The treatment conditions described above were also used for the analysis of GFP-ATG8a
127 (CS39996), ER-GFP (CS16251), and *bzip60* (CS813074) (all three plant lines were obtained from
128 ABRC (Arabidopsis Biological Resource Center). The *ire1a/b* line was kindly provided by Chen et al.,
129 2013 and Pu et al., 2019. The homozygous *hsfa1a/b/d* (psi00284) line was obtained from RIKEN-BRC.

130 **Phenotypic analysis**

131 To determine the effect of priming or triggering heat stress on growth, seedlings were analysed for leaf
132 number, root length and fresh weight. Data for leaf number (48 seedlings from three independent
133 experiments), primary root length (18 seedlings from three independent experiments) and fresh weight
134 (three biological replicates, where one replicate includes 16 seedlings) were collected and analysed.
135 Root length was measured using the ImageJ software (https://imagej.net/software/fiji/) (Schneider et
136 al., 2012).

137 **Protein extraction and Western blot analysis**

138 Soluble protein was extracted from five-day-old *Arabidopsis* seedlings as previously described in
139 Yamamoto et al. (2018) with a few modifications. About 40-50 mg of seedlings were collected and
140 frozen in liquid nitrogen. The samples were ground using Retsch Miller MM400 at 25Hz for 30 seconds
141 (s) (x2 cycles). After grinding, 200-300µl of 1x RIPA lysis buffer (Merck; 20-188) containing 10%
142 glycerol, 1x phosphatase inhibitor cocktail (PhosSTOP, Roche; 4906837001), and 1x protease inhibitor
143 cocktail (Roche; 4693132001) was added and incubated at 4°C for 1 h at 1500 rpm. The samples were
144 centrifuged at 14000 rpm for 30 min at 4°C, after which the supernatant containing protein was collected
145 and stored at -80°C until further use. Plant protein aggregates were extracted using a standard protocol

146 as described by Phukan et al. (2023).

147 For protein analysis, protein concentration was estimated using the BCA method, following the
148 manufacturer's instructions (Cat. No. 23225). Protein (20 µg per lane) was loaded onto an 8% SDS-
149 PAGE gel, which was stained using Coomassie Brilliant Blue. Protein bands were visualized after
150 destaining the gel following a standard protocol ("Destaining Solution for Coomassie Brilliant Blue
151 R250," 2007). For Western blot analysis, 20 µg of protein was loaded onto 6-12% SDS-PAGE,
152 following which the proteins were transferred to the nitrocellulose membrane. The blot was blocked
153 using 5% BSA or 2% skim milk solution for 1 h at room temperature (RT), followed by primary
154 antibody incubation (overnight at 4°C). The blot was developed after secondary antibody incubation (1
155 h at RT) using Immobilon Forte HRP substrate (Cat. No. WBLUF0500). α-Tub (CST 3873), ATG8
156 (Abcam, ab77003), ATG8 (Agrisera, AS14 2769), GFP (CST 2956), HSP70 (Abcam, ab2787), HSP90
157 (Sigma, CA1023), HSP90 (Agrisera, AS08 346), HSP17.6 (Agrisera, AS07 254), HSP21 (Agrisera,
158 AS08 285), HSP101 (Agrisera, AS08 287), pS6K (CST 9234), S6K (CST 9202), pAMPK-α (CST
159 2535), Ubiquitin (CST 3933) and Actin (AS13 2640) were used as primary antibodies. Anti-rabbit (sc-
160 2313; CST 7074) and anti-mouse (CST 7076) were used as secondary antibodies. Blots were quantified
161 densitometrically using ImageJ software (https://imagej.net/software/fiji/).

162 **Gene expression analysis**

163 For gene expression analysis, about 40-50 mg of five-day-old *Arabidopsis* seedlings were collected at
164 several time points (post-priming and triggering, and during recovery) and frozen in liquid nitrogen.
165 The samples were ground using Retsch Miller MM400 at 25Hz for 30 s (x2 cycles). After grinding,
166 RNA was isolated from the samples using a combination of TRIzol/chloroform extraction and kit
167 method (PureLink™ RNA Mini Kit, Thermo; 12183018A). The purified RNA was treated with DNase
168 I (NEB; M0303) following standard protocol. cDNA was synthesized using 1 µg of RNA following
169 manufacturer's instructions (1st strand cDNA synthesis kit, Takara; 6110A). RT-PCR was performed
170 using SapphireAmp® Fast PCR Master Mix (Takara; RR350A), while iTaq™ Universal SYBR® Green
171 Supermix (Biorad; 1725121) was used for performing qRT-PCR. Gene accession IDs and PCR primers
172 are described in **Table S1**.

173 **Microscopy**

174 The primed and unprimed ER-GFP seedlings were collected post-triggering heat stress and fixed using

175 4% paraformaldehyde solution (Himedia; TCL119) containing 0.1% Triton X-100 (Zhu et al., 2020).
176 After adding the fixating solution, the samples were kept in a desiccator for 30-40 seconds by applying
177 vacuum. The process was repeated several times until the seedlings sank. The samples were then
178 incubated with shaking in a fixating solution for 20 min, followed by washing with 1xPBS (3 times) for
179 5 min. *Arabidopsis* leaf tissue was visualized under 40x magnification using Zeiss LSM 710 confocal
180 microscope. A total of 16 seedlings from four independent experiments were imaged for each time
181 point. Images were analysed using ImageJ software (https://imagej.net/software/fiji/).

182 **Statistical Analysis**

183 The data was plotted using GraphPad Prism 10.0 (https://www.graphpad.com/). The experiments were
184 conducted using three biological replicates unless stated otherwise. The data was analysed using One-
185 way ANOVA (for qPCR data), Two-way ANOVA and student's t-test (for phenotype analysis) to obtain
186 statistical significance. p values <0.05 were considered significant (**Dataset S1 and S2**).

187 ## Results

188 **Priming improves survival from severe heat stress**

189 To understand the mechanism driving short-term acquired thermotolerance, we exposed the five-day-
190 old Arabidopsis wild-type (WT) seedlings to 37°C (for 90 min) and allowed them to briefly recover at
191 optimum conditions (for 90 min) before exposing them to triggering heat stress (45°C for 45 min)
192 (**Figure 1A**). Hereafter, this condition is referred to as 'primed'. The effect of thermopriming was
193 analysed by comparing the impact of lethal heat stress on primed *vs.* naive (unprimed: directly exposed
194 to triggering heat stress) seedlings. Post heat stress, we recorded the seedling growth as a function of
195 time under all the conditions tested (control, primed and unprimed) (**Figure 1B**). Post-exposure to
196 triggering heat stress, primed seedlings displayed a halt in growth; however, the growth resumed
197 quickly, which was found to be significantly higher than the unprimed, quantified as leaf number, root
198 length and fresh weight (**Figure 1, C-E**). Five days post heat stress, unprimed seedlings display a visibly
199 complete loss of chlorophyll and fail to survive (**Figure 1B**). To summarise, heat stress affects growth
200 in both primed and unprimed conditions. However, primed plants can mount a better response, aiding
201 in resuming growth swiftly post-heat stress.

202 **Thermopriming mitigates heat stress-induced protein damage**

203 To determine whether priming-mediated seedling survival upon heat stress is associated with efficient
204 maintenance of proteins, we analysed the total protein content in heat-treated/untreated seedlings across
205 all conditions (**Figure 2A**). The protein content in the control (grown at optimal conditions at 22°C),
206 primed control (subjected to only priming stimulus at 37ºC and returned to optimal conditions) and
207 primed seedlings was found to be similar across all the time points analysed post-heat stress (**Figure**
208 **2B**). On the other hand, unprimed seedlings display a consistent drop in total protein levels from 1 to 3
209 days post stress (DPS), indicating a loss in total protein content (**Figure 2B**). These results suggest that
210 priming-mediated heat stress tolerance may involve efficient maintenance of the protein
211 pool/homeostasis.

212 **Priming modulates proteostasis through temporal regulation of autophagy and chaperones**

213 We next assessed the status of protein homeostasis maintenance pathways – autophagy and chaperone
214 response during the heat stress paradigm. We analysed chaperone levels (HSP70 and HSP90) post-heat
215 stress across all conditions. Exposure to the priming stimulus (AP) results in increased accumulation of
216 HSP70 and HSP90, which persists until 1 DPS post-exposure to triggering heat stress in the primed
217 compared to the control (**Figure 2, C and D**). However, the unprimed seedlings fail to mount such a
218 response, with the levels of HSPs being lower than the control seedlings (**Figure 2, C and D**). In
219 addition, we analysed the abundance of other heat stress inducible proteins HSP17.6, HSP21 and
220 HSP101 (Bäurle, 2016; Friedrich et al., 2021) at all the time points stated above. Increased levels of all
221 three HSPs were detected in the primed, but not in the unprimed or control seedlings (**Figure 2, E and**
222 **F**). Immediately upon exposure to priming (AP), an increased abundance of HSP17.6, HSP21 and
223 HSP101 was detected (**Figure 2E**), which persisted until 3 DPS (**Figure 2F**). HSP101 and HSP17.6
224 were retained longer compared to HSP21 in the primed control (**Figure 2F**). Furthermore, to assess
225 whether the HSP abundance observed thus far parallels transcript levels across all conditions, we
226 profiled the expression of these *HSPs* (**Figure 2G**). In the primed seedlings, the abundance of HSPs
227 correlated with their elevated transcript levels compared to those of the control. Surprisingly, unprimed
228 seedlings displayed a gradual increase in *HSPs* transcript abundance post-heat stress (**Figure 2G**),
229 which does not correlate with the protein levels observed (**Figure 2, C-F**). Nonetheless, primed controls
230 display increased *HSP* expression, which gradually declines with time (**Figure 2G**).

231 We next quantified the autophagy response post-heat stress by using ATG8 as a marker. ATG8 is an
232 autophagosome membrane protein crucial for autophagosome formation (Shpilka et al., 2011), and

233 elevated ATG8 levels correlate with increased autophagy (Upadhyaya et al., 2020). We observed that
234 exposure to the priming temperature itself could induce autophagy (**Figure 3A**). However, immediately
235 post-exposure to triggering heat stress (0h), ATG8-PE levels increased in both unprimed and primed
236 seedlings compared to the control (**Figure 3A**). To assess if the heat stress-induced autophagy sustains,
237 declines or surges with time, we checked the ATG8 levels from 1 to 3 DPS. In the unprimed seedlings,
238 the ATG8-PE levels increased further by 1 DPS, which continued until 2 DPS (**Figure 3B**). Notably,
239 the visible decline in ATG8 levels (at 3 DPS) correlates with the reduced protein content in the unprimed
240 seedlings (**Figure 2B**). However, in the primed seedlings, ATG8-PE levels declined by 1 DPS to levels
241 comparable to the control (**Figure 3B**). No difference in ATG8 levels was detected in the primed control
242 compared to the control (**Figure 3B**). An increase and decrease in ATG8-PE levels in the unprimed *vs.*
243 primed, respectively, by 1 DPS, suggests dynamic regulation of autophagy in the primed seedlings
244 between 0 and 1 DPS. We also measured the autophagy flux across our paradigm using the GFP-ATG8
245 processing assay (Kang et al., 2018; Shin et al., 2014). Autophagy flux, as measured by free-GFP to
246 total-GFP ratio, was high in unprimed, indicating highly active autophagy compared to primed and
247 control, post-heat stress (**Figure 3, C and D**). Such a decrease or increase/sustenance of autophagy in
248 the primed *vs.* unprimed, respectively, suggests priming-mediated dynamic regulation of autophagy.

249 Our findings indicate that priming-mediated heat stress tolerance involves the accumulation of HSPs
250 and dynamic activation of autophagy, which may contribute to the effective maintenance of protein
251 homeostasis under stress. To test this, we examined the proteostasis state by analysing for ubiquitin-
252 conjugated protein aggregates at 1 DPS, the time at which we observed differential autophagy between
253 the primed and unprimed conditions (**Figure 3B**). The unprimed seedlings displayed elevated ubiquitin-
254 conjugated aggregates compared to primed or control (**Figure 3, E and F**). Collectively, these findings
255 suggest that priming aids in the timely activation of chaperone and autophagy responses to maintain
256 protein homeostasis, thereby enhancing plant heat stress tolerance. In contrast, unprimed seedlings
257 display sustained autophagy with very low to undetectable HSP levels, resulting in perturbed
258 proteostasis and fail to survive.

259 **Regulation of autophagy under heat stress is TOR and SnRK-independent**

260 Previous studies have identified the role of TOR and SnRK in the regulation of autophagy under stress
261 (Pu et al., 2017; Soto-Burgos & Bassham, 2017; Yang et al., 2023). We wondered if TOR/SnRK are
262 involved in the priming-mediated regulation of autophagy under heat stress. To test this, we analysed

263 the phospho-S6K (pS6K) levels as a measure of TOR kinase activity (Raught et al., 2001; Upadhyaya
264 et al., 2020) and active-SnRK (pAMPK: using phospho-AMPKα antibody) for SnRK activity (Baena-
265 González et al., 2007; Belda-Palazón et al., 2020). Interestingly, neither pS6K **(Figure S1, A-D)** nor the
266 pAMPK levels **(Figure S1, E-H)** were altered at any of the time points across all the conditions. These
267 findings suggest that priming- and heat stress-mediated regulation of autophagy (as observed in **Figure**
268 **3, A-B**) is independent of TOR and SnRK.

269 **Unprimed seedlings exhibit sustained ER stress**

270 We next checked if the abrogated accumulation of HSPs in the unprimed seedlings is associated with
271 the endoplasmic reticulum (ER) stress, as dysregulation in protein homeostasis is known to impact ER
272 functional status (Humbert et al., 2012). The IRE1 protein is involved in the maintenance of proteostasis
273 in the ER (Nawkar et al., 2018; Pastor-Cantizano et al., 2020). Upon stress, IRE1 activation leads to the
274 splicing of *bZIP60u* (unspliced), forming *bZIP60* spliced form (*bZIP60s*), which is known to
275 transcriptionally modulate genes involved in unfolded protein response (Bao et al., 2018; Deng et al.,
276 2011; Humbert et al., 2012). To examine the ER stress levels, if any, we analysed the transcript
277 abundance of *bZIP60s* across all the conditions at different time points post-priming/triggering stress.
278 Interestingly, exposure to priming temperature itself triggered ER stress (*bZIP60s* form visible at AP;
279 **Figure 4A**). Post-triggering heat stress, although primed seedlings display ER stress initially (AT/0
280 DPS), they recover by 1 DPS (**Figure 4, A and B; S2A**). In contrast, the unprimed seedlings display
281 elevated and sustained *bZIP60s* levels post-exposure to triggering heat stress, suggesting high ER stress
282 (**Figure 4, A and B; S2A**) compared to the control (*bZIP60s* undetectable).

283 To further examine the ER status, we used an ER-specific GFP marker as a visual marker (Nelson et
284 al., 2007). In the unprimed, GFP signal was visible immediately post-triggering heat stress (0 DPS),
285 which dramatically reduced to undetectable levels from 1 to 3 DPS (**Figure S2B**). Contrarily, the primed
286 seedlings display the ER-GFP signal similar to that of the control at all the time points tested. These
287 results suggest that priming aids in the efficient maintenance of ER under heat stress, which is absent
288 in the unprimed, potentially resulting in the disruption of the ER. Taken together, these findings indicate
289 that thermopriming mitigates the heat stress-induced ER stress, promoting seedling survival.

290 **ER-associated IRE1 modulates autophagy during priming**

291 In addition to regulating *bZIP60* splicing, IRE1 also modulates autophagy by fine-tuning the RIDD

292 (Regulated IRE1-dependent decay of mRNA) activity (Li & Howell, 2021; Maurel et al., 2014).
293 Notably, RIDD leads to the downregulation of inhibitors of autophagy, such as *BGLU21*, *ROSY1* and
294 *PR-14,* by targeting those mRNAs for degradation (Bao et al., 2018). We surmised that reversal to basal
295 level *vs.* more sustained autophagy in the primed and unprimed, respectively, may involve RIDD-
296 mediated regulation. Therefore, we examined *BGLU21*, *ROSY1* and *PR-14* transcript levels across all
297 the conditions and time points tested. At the time points- post priming (AP), before triggering (BT) and
298 after triggering (AT: 0 DPS), primed seedlings showed a significant reduction in the transcript levels of
299 all three genes compared to the control (**Figure 4, C-E**). However, by 1-2 DPS, we observed a recovery
300 in their transcript abundance (**Figure 4, C-E**). Contrary to this, the transcript levels of *BGLU21* and
301 *PR14* significantly remained lower in unprimed seedlings at all the time points compared to the control
302 (**Figure 4, C-E**). Whereas, except for *BGLU21* after triggering stress time-point, no significant
303 difference in transcript abundance was observed in the primed control compared to control seedlings
304 (**Figure 4, C-E**). Particularly, these changes in the transcript abundance correlate with the
305 ATG8/ATG8-PE levels in these seedlings (**Figure 3, A-B**). For instance, in the primed, reduced
306 transcript abundance of these autophagy inhibitors correlates with the induced autophagy (at AP, BT,
307 AT). By 1-2 DPS, when the transcript abundance of these inhibitors reverts to near control level (**Figure**
308 **4, C-E**), autophagy was found to return to basal level in the primed (**Figure 3, A-B**). Contrarily,
309 sustained induction of autophagy aligns with reduced transcript abundance of the autophagy inhibitors
310 in the unprimed, post-exposure to triggering heat stress (**Figure 3, A-B; Figure 4, C-E**). These
311 observations suggest that priming modulates autophagy, potentially through the IRE1-RIDD-mediated
312 regulation.

313 **Loss of bZIP60 or IRE1 leads to a delay in priming-mediated heat stress recovery**

314 We next analysed the response of *bzip60* and *ire1a ire1b* (referred to as *ire1a/b*) homozygous mutants
315 (**Figure S3, A-B**) to heat stress with or without priming. When directly exposed to triggering heat stress
316 (unprimed), both *bzip60* and *ire1a/b* seedlings failed to survive (**Figure S3, C-D**), which was similar to
317 wild-type (WT) (**Figure 1B**). However, the growth of primed seedlings was found to be slower in the
318 mutants. When observed seven days post heat stress, the root length was found to be significantly lower
319 in the primed *bzip60* and *ire1a/b* compared to their respective control, while the root length of primed
320 WT was found to be similar to that of its control (**Figure 5A**).

321 Further, we assessed whether the autophagy dynamics are affected in the *bzip60* and *ire1a/b* mutants

322 upon exposure to heat stress. We observed that the autophagy was induced in the *bzip60* and *ire1a/b*
323 mutants (**Figure S4, A-B**) and its dynamics remain similar to that of WT (**Figure 3, A-B**). Loss of
324 IRE1A/B and bZIP60 did not seem to disrupt autophagy induction during heat stress. This was
325 surprising as we observed thus far that high temperature induces ER stress, which activates IRE1,
326 thereby regulating autophagy. However, autophagy was still being induced in the absence of IRE1A/B
327 and bZIP60. These findings suggest a partial role for IRE1-bZIP60 and may involve alternate autophagy
328 regulatory mechanisms operating during heat stress.

329 We next analysed the HSP levels in *bzip60* and *ire1a/b* mutants. Primed *bzip60* and *ire1a/b* seedlings
330 display elevated levels for all the HSPs tested (**Figure 5B**). However, slight differences still exist in the
331 abundance of HSPs across genotypes. For instance, HSP17.6 and HSP21 show similar induction
332 patterns across WT and *ire1a/b*, wherein both the HSPs reach maximal induction by 1 DPS, whereas
333 the *bzip60* mutant displayed a maximum level of HSP21 at 2 DPS (**Figure 5C**). Nonetheless, primed
334 WT shows a slightly higher abundance of both HSP17.6 and HSP21 at 0 DPS compared to *bzip60* and
335 *ire1a/b*. Similarly, both mutants displayed differences in the induction of HSP70 and HSP101 compared
336 to WT. For HSP70, the level of induction in the mutants and WT was minimal at all the time points
337 tested (**Figure 5C**). However, HSP101 was highest in WT compared to the mutants at 0 DPS post-heat
338 stress, which declined from 0 to 3 DPS. Both the mutants displayed the highest abundance only at 1
339 DPS, while *bzip60* showed a steady decline from 1 to 3 DPS (**Figure 5C**). The unprimed *bzip60* and
340 *ire1a/b* displayed no detectable level of HSPs (**Figure 5B**), similar to the unprimed WT. To assess if
341 the protein level changes parallel transcript level changes, we determined the *HSPs* expression in both
342 mutants. As expected, all the *HSPs* tested displayed elevated transcript levels post-priming in both
343 *bzip60* and *ire1a/b* (**Figure 5D**). Unprimed *bzip60* and *ire1a/b* also displayed a delayed increase in *HSP*
344 transcript levels (**Figure 5D**), similar to WT (**Figure 2G**).

345 **Activation of the protein protective response is crucial for heat stress tolerance**

346 As we posit that alternate mechanisms may operate to regulate autophagy, we looked at HSFA1a, a
347 transcription factor previously shown to induce autophagy under abiotic stress conditions (Wang et al.,
348 2015; Xie et al., 2022). To examine if HSFA1 is involved, we first assessed if it is active during the
349 priming/triggering regime. The HSFA1-mediated response is primarily executed through the induction
350 of its downstream targets *HSFA2* and *HSFA3* (Friedrich et al., 2021; Ohama et al., 2017). Therefore,
351 we profiled the expression levels of *HSFA1a*, *HSFA2,* and *HSFA3* post-priming/triggering heat stress.

352 We observed that *HSFA1a* levels do not significantly change, except at the AT/1DPS timepoint in
353 unprimed, across the time points tested (**Figure 6A**). Our observations were in line with previous reports
354 where *HSFA1a* levels did not significantly change under ER stress (Löchli et al., 2023), likely because
355 HSFA1 regulation under heat stress is predominantly controlled at the post-translational level
356 (Mesihovic et al., 2022; Ohama et al., 2017; Wang et al., 2023). In contrast, the downstream targets
357 *HSFA2* and *HSFA3* were upregulated in both primed and unprimed following heat stress (**Figure 6A**).
358 Notably, *HSFA2* induction persisted even at 2 DPS, whereas *HSFA3* induction returned to basal levels
359 by 1 DPS in primed seedlings (**Figure 6A**).

360 To overcome the functional redundancy of the HSFA1s in *Arabidopsis*, we used a previously reported
361 *hsfa1a/b/d* triple mutant line (Yoshida et al., 2011) for our analysis. The unprimed *hsfa1a/b/d* and Col-
362 0/Ws-0 did not show any difference in their heat stress response (**Figure 6B**). However, even upon
363 priming, the *hsfa1a/b/d* mutants failed to display survival post-heat stress, unlike the Col-0/Ws-0
364 seedlings (**Figure 6B**). When we probed to assess autophagy in *hsfa1a/b/d*, we observed that autophagy
365 remains highly induced in both primed and unprimed, even after 2-3 DPS (**Figure 6C**). Moreover, the
366 priming-mediated HSP induction was abolished in the *hsfa1a/b/d* mutant in contrast to WT (**Figure**
367 **6D**).

368 These observations suggest that the absence of protein protective response (chaperone), as seen in
369 unprimed (all genotypes) and primed (*hsfa1a/b/d* mutant), leads to persistent activation of clearance
370 response (autophagy) to resolve proteotoxic stress, but ultimately leads to lethality. Taken together, our
371 study identifies that timely modulation of protein homeostasis through the accumulation of HSP and
372 activation of autophagy underpins heat stress tolerance following thermopriming. While IRE1 is
373 involved in the regulation of the priming response, HSFA1 is crucial in determining the priming-
374 mediated heat stress response outcomes.

375 Discussion

376 In the current study, we demonstrate that efficient regulation of protein homeostasis underlies priming-
377 mediated short-term acquired thermotolerance in *Arabidopsis thaliana*. Heat stress exerts a profound
378 impact on the thermolabile molecular complexes, resulting in protein dysfunction and aggregation
379 (McLoughlin et al., 2019; Mittler et al., 2012; Rosenzweig et al., 2019). Maintaining proteostasis under
380 stress requires a fine balance between timely refolding of proteins via robust chaperone activity and the

381 efficient clearance of irreversibly damaged proteins through the action of disaggregases, autophagy, or
382 the UPS (Hartl et al., 2011; McLoughlin et al., 2019; Mogk et al., 2018). Disruption of this balance can
383 lead to proteotoxic stress, ultimately compromising cellular viability. In this study, we observed that
384 direct exposure to heat stress severely impacts protein content in the unprimed seedlings, which is
385 alleviated in the primed seedlings. These observations are consistent with the previous reports showing
386 that protein content reduces upon exposure to noxious heat stress (Gulen & Eris, 2004; Nagy-Réder et
387 al., 2022). We found that thermopriming facilitates a dynamic autophagy response (quantified as ATG8-
388 PE levels and RIDD target expression) alongside an increase in chaperone abundance, which together
389 contribute to the maintenance of protein homeostasis. Previous reports on long-term acquired
390 thermotolerance also observed autophagy to be induce post-priming stimulus (Sedaghatmehr et al.,
391 2019, 2021).

392 Contrastingly, unprimed seedlings display induced autophagy even at 2 DPS, and fail to accumulate
393 HSPs at the protein level despite a significant expression at the transcript level. We posit that such
394 failure may stem from either HSP sequestration within aggregates or impaired translation post-stress.
395 Notably, HSP101, a critical disaggregase that coordinates with other HSPs to resolve proteotoxic stress
396 (McLoughlin et al., 2019), was detected only in the primed condition (**Figure S5**). This suggests that
397 the chaperone protein is likely not synthesized in the unprimed seedlings upon heat stress. In addition,
398 the unprimed seedlings displayed high levels of ubiquitinylated insoluble proteins, a trend also reported
399 in HSP101 deficient plants during heat stress (McLoughlin et al., 2019). Priming has also been shown
400 to protect the global translational potential under heat stress, whereas direct heat exposure leads to
401 preferential co-translational decay of ER-translated mRNAs (Dannfald et al., 2025). Together, these
402 findings underscore the importance of maintaining a delicate balance between protein -folding and -
403 clearance machineries to restore cellular homeostasis following stress. In unprimed seedlings, the
404 collapse of this balance, as evidenced by failure to accumulate chaperones, aggregate buildup, and
405 excessive autophagy, impacts their growth and survival.

406 Given the difference in autophagy response between primed and unprimed, we examined the role of
407 TOR/SnRK-dependent pathways, previously known to be involved in regulating autophagy (Signorelli
408 et al., 2019; Soto-Burgos & Bassham, 2017; Yang et al., 2023), However, we did not detect any changes
409 in TOR/SnRK activity under our thermopriming/heat stress regime, suggesting that alternative
410 pathways might be at play. Indeed, TOR-independent mechanisms have been reported to modulate

411 autophagy during oxidative and ER stress conditions (Pu et al., 2017). Since we observed
412 thermopriming to induce ER stress, we explored the potential involvement of IRE1. IRE1-RIDD activity
413 has been previously associated with autophagy induction under tunicamycin treatment (ER-stress
414 inducing agent), wherein RIDD-mediated degradation of autophagy inhibitors was shown to promote
415 autophagy (Bao et al., 2018). Findings from this study show that thermopriming facilitates the dynamic
416 degradation of RIDD target transcripts, which correlate with the induction of autophagy in primed
417 seedlings. Similarly, in unprimed, the prolonged autophagy induction was associated with sustained
418 downregulation of autophagy inhibitors. While these observations suggest that RIDD activity influences
419 autophagy by modulating the abundance of specific inhibitors, the precise mechanism remains to be
420 explored. Bao et al. (2018) suggests that BGLU21 (β-glucosidase 21), ROSY1 (interactor of
421 synaptotagmin 1), and PR-14 (pathogenesis-related protein 14) proteins might interfere with the
422 lipidation of ATG8, a crucial step for autophagosome formation, thereby affecting autophagy.

423 Furthermore, analysis of the *bzip60* and *ire1a/b* knockout mutants under primed conditions revealed
424 reduced growth recovery post-stress compared to WT. Although primed *bzip60* and *ire1a/b* seedlings
425 displayed an increase in HSP levels, their response was delayed compared to WT. This aligns with
426 earlier findings that *ire1a/b* mutants exhibit severe growth retardation and attenuated protein translation
427 under ER stress, effects that could be mitigated by synthetic chaperones (Pu et al., 2019; Yoo et al.,
428 2024). Notably, despite the loss of IRE1A/B or bZIP60, autophagy induction was still observed post-
429 heat stress. This concurs with the previous report that shows bZIP60 to be dispensable for IRE1-
430 dependent autophagy induction during ER stress (Bao et al., 2018), and *ire1b* mutants can induce
431 autophagy following 42°C heat treatment (Yang et al., 2016). As *ire1b* and *ire1a/b* have been shown
432 not to induce autophagy under ER stress from DTT or tunicamycin (Bao et al., 2018; Liu et al., 2012)
433 and given that autophagy was still activated in *ire1a/b*, we suggest that alternative regulatory pathways
434 may mediate heat-induced autophagy.

435 One such potential regulator is HSFA1a, a transcriptional activator of autophagy in tomato under heat
436 and drought stress (Löchli et al., 2023; Wang et al., 2015; Xie et al., 2022). We found that HSFA1a
437 remains highly active in our paradigm, as its downstream targets *HSFA2* and *HSFA3* are significantly
438 induced following heat stress. However, we observed that in the *hsfa1a/b/d* mutant, autophagy remains
439 highly induced in both primed and unprimed, even at 2-3 DPS. Previous studies have implicated the
440 involvement of NBR1 (next-to-BRCA1) and ATI3 (ATG8-interacting 3) for autophagy response under

441 heat stress (Jung et al., 2020; Thirumalaikumar et al., 2020; Zhou et al., 2018), suggesting that
442 autophagy response involves multilayered regulation, a feature advantageous for sessile organisms to
443 tackle challenging environments. Moreover, the *hsfa1a/b/d* mutant fails to survive heat stress even upon
444 exposure to a priming stimulus, unlike Col-0/Ws-0. Such failure to mount the priming-mediated
445 response to heat stress could be due to the inability to induce HSPs, implying that efficient protein
446 maintenance (by chaperones) is a critical determinant towards stress response outcomes. An earlier
447 report suggested that autophagy contributes to the degradation of HSP, as autophagy mutants showed
448 prolonged chaperone accumulation (Sedaghatmehr et al., 2019). However, our findings indicate that
449 autophagy and chaperone response may act cooperatively to modulate protein homeostasis, with the
450 impairment of one pathway potentially amplifying the activity of the other to mitigate proteotoxic stress.

451 In conclusion, our study highlights that the efficient maintenance of protein homeostasis through the
452 accumulation of chaperones and dynamic autophagy response evoked by thermopriming, aids in
453 seedling survival and growth upon heat stress (**Figure 7**). In the absence of priming, this balance is
454 disrupted, leading to a dysregulation of proteostasis and ultimately seedling death. Further, we identify
455 that IRE1-mediated regulation operates during thermopriming, but it is not essential. However, HSFA1
456 is indispensable for mounting priming-mediated heat stress tolerance. Collectively, these findings
457 reveal that precise and coordinated regulation of protein folding and clearance pathways is a key
458 determinant of thermotolerance in *Arabidopsis thaliana*.

459 ## Acknowledgements

460 MB acknowledges the Council of Scientific and Industrial Research (CSIR), Govt. of India, for his
461 fellowship. This work was supported by funding from the Department of Science and Technology (Sir
462 JC Bose Fellowship – for BJR), Science and Engineering Research Board (SPG/2021/004000) and
463 intramural support from IISER Tirupati (ADA and BJR), University of Hyderabad (BJR). We express
464 our sincere gratitude to Prof. Diane Bassham (Iowa State University) and Prof. Federica Brandizzi
465 (Michigan State University) for providing us with seeds of *ire1a ire1b* mutant.

466 ## Authors Contribution

467 **MB:** Designing the experiments, performing the experiments, interpretation of results, preparation of
468 the figures, writing the manuscript; **ADA:** conceptualization of the research question, supervising the

work, designing the experiments, interpretation of results, writing and editing the manuscript, funding acquisition; **BJR:** conceptualization of the research question, supervising the work, designing the experiments, interpretation of results, writing and editing the manuscript, funding acquisition.

Competing Interests

The authors have no competing interest.

References

Baena-González, E., Rolland, F., Thevelein, J. M., & Sheen, J. (2007). A central integrator of transcription networks in plant stress and energy signalling. *Nature 2007 448:7156*, *448*(7156), 938–942. https://doi.org/10.1038/nature06069

Balmer, A., Pastor, V., Glauser, G., & Mauch-Mani, B. (2018). Tricarboxylates induce defense priming against bacteria in arabidopsis thaliana. *Frontiers in Plant Science*, *9*, 1221. https://doi.org/10.3389/FPLS.2018.01221/BIBTEX

Bao, Y., Pu, Y., Yu, X., Gregory, B. D., Srivastava, R., Howell, S. H., & Bassham, D. C. (2018). IRE1B degrades RNAs encoding proteins that interfere with the induction of autophagy by ER stress in Arabidopsis thaliana. *Autophagy*, *14*(9), 1562–1573. https://doi.org/10.1080/15548627.2018.1462426/SUPPL_FILE/KAUP_A_1462426_SM0835.DOCX

Bäurle, I. (2016). Plant Heat Adaptation: priming in response to heat stress. *F1000Research 2016 5:694*, *5*, 694. https://doi.org/10.12688/f1000research.7526.1

Belda-Palazón, B., Adamo, M., Valerio, C., Ferreira, L. J., Confraria, A., Reis-Barata, D., Rodrigues, A., Meyer, C., Rodriguez, P. L., & Baena-González, E. (2020). A dual function of SnRK2 kinases in the regulation of SnRK1 and plant growth. *Nature Plants 2020 6:11*, *6*(11), 1345–1353. https://doi.org/10.1038/s41477-020-00778-w

Catoni, M., Alvarez-Venegas, R., Worrall, D., Holroyd, G., Barraza, A., Luna, E., Ton, J., & Roberts, M. R. (2022). Long-Lasting Defence Priming by β-Aminobutyric Acid in Tomato Is Marked by Genome-Wide Changes in DNA Methylation. *Frontiers in Plant Science*, *13*, 1071. https://doi.org/10.3389/FPLS.2022.836326/BIBTEX

Chen, Y., Aung, K., Rolčík, J., Walicki, K., Friml, J., & Brandizzi, F. (2013). INTER-REGULATION OF THE UNFOLDED PROTEIN RESPONSE AND AUXIN SIGNALING. *The Plant Journal : For Cell and Molecular Biology*, *77*(1), 97. https://doi.org/10.1111/TPJ.12373

Conrath, U. (2011). Molecular aspects of defence priming. *Trends in Plant Science*, *16*(10), 524–531. https://doi.org/10.1016/J.TPLANTS.2011.06.004

Conrath, U., Beckers, G. J. M., Flors, V., García-Agustín, P., Jakab, G., Mauch, F., Newman, M. A., Pieterse, C. M. J., Poinssot, B., Pozo, M. J., Pugin, A., Schaffrath, U., Ton, J., Wendehenne, D., Zimmerli, L., & Mauch-Mani, B. (2007). Priming: Getting Ready for Battle. *Http://Dx.Doi.Org/10.1094/MPMI-19-1062*, *19*(10), 1062–1071. https://doi.org/10.1094/MPMI-19-1062

Crespo-Salvador, Ó., Escamilla-Aguilar, M., López-Cruz, J., López-Rodas, G., & González-Bosch, C. (2018). Determination of histone epigenetic marks in Arabidopsis and tomato genes in the early

response to Botrytis cinerea. *Plant Cell Reports*, *37*(1), 153–166. https://doi.org/10.1007/S00299-017-2218-9/FIGURES/6

Dannfald, A., Carpentier, M.-C., Merret, R., Favory, J.-J., & Deragon, J.-M. (2025). Plant response to intermittent heat stress involves modulation of mRNA translation efficiency. *Plant Physiology*, *197*(2), 648. https://doi.org/10.1093/PLPHYS/KIAE648

Deng, Y., Humbert, S., Liu, J. X., Srivastava, R., Rothstein, S. J., & Howell, S. H. (2011). Heat induces the splicing by IRE1 of a mRNA encoding a transcription factor involved in the unfolded protein response in Arabidopsis. *Proceedings of the National Academy of Sciences of the United States of America*, *108*(17), 7247–7252. https://doi.org/10.1073/PNAS.1102117108/SUPPL_FILE/PNAS.201102117SI.PDF

Destaining solution for Coomassie brilliant blue R250. (2007). *Cold Spring Harbor Protocols*, *2007*(2), pdb.rec10717. https://doi.org/10.1101/PDB.REC10717

Espinas, N. A., Saze, H., & Saijo, Y. (2016). Epigenetic control of defense signaling and priming in plants. *Frontiers in Plant Science*, *7*(AUG2016), 1201. https://doi.org/10.3389/FPLS.2016.01201/BIBTEX

Fahad, S., Bajwa, A. A., Nazir, U., Anjum, S. A., Farooq, A., Zohaib, A., Sadia, S., Nasim, W., Adkins, S., Saud, S., Ihsan, M. Z., Alharby, H., Wu, C., Wang, D., & Huang, J. (2017). Crop production under drought and heat stress: Plant responses and management options. *Frontiers in Plant Science*, *8*, 1147. https://doi.org/10.3389/FPLS.2017.01147/BIBTEX

Friedrich, T., Oberkofler, V., Trindade, I., Altmann, S., Brzezinka, K., Lämke, J., Gorka, M., Kappel, C., Sokolowska, E., Skirycz, A., Graf, A., & Bäurle, I. (2021). Heteromeric HSFA2/HSFA3 complexes drive transcriptional memory after heat stress in Arabidopsis. *Nature Communications*, *12*(1). https://doi.org/10.1038/s41467-021-23786-6

Gamir, J., Sánchez-Bel, P., & Flors, V. (2014). Molecular and physiological stages of priming: how plants prepare for environmental challenges. *Plant Cell Reports*, *33*(12), 1935–1949. https://doi.org/10.1007/S00299-014-1665-9

Gao, C., Peng, X., Zhang, L., Zhao, Q., Ma, L., Yu, Q., Lian, X., Gao, L., Xiong, L., & Li, S. (2023). Proteome and Ubiquitylome Analyses of Maize Endoplasmic Reticulum under Heat Stress. *Genes*, *14*(3), 749. https://doi.org/10.3390/GENES14030749/S1

Gulen, H., & Eris, A. (2004). Effect of heat stress on peroxidase activity and total protein content in strawberry plants. *Plant Science*, *166*(3), 739–744. https://doi.org/10.1016/J.PLANTSCI.2003.11.014

Hartl, F. U., Bracher, A., & Hayer-Hartl, M. (2011). Molecular chaperones in protein folding and proteostasis. *Nature*, *475*(7356), 324–332. https://doi.org/10.1038/nature10317

Humbert, S., Zhong, S., Deng, Y., Howell, S. H., & Rothstein, S. J. (2012). Alteration of the bZIP60/IRE1 Pathway Affects Plant Response to ER Stress in Arabidopsis thaliana. *PLOS ONE*, *7*(6), e39023. https://doi.org/10.1371/JOURNAL.PONE.0039023

Jung, H., Lee, H. N., Marshall, R. S., Lomax, A. W., Yoon, M. J., Kim, J., Kim, J. H., Vierstra, R. D., & Chung, T. (2020). Arabidopsis cargo receptor NBR1 mediates selective autophagy of defective proteins. *Journal of Experimental Botany*, *71*(1), 73–89. https://doi.org/10.1093/JXB/ERZ404

Kang, S., Shin, K. D., Kim, J. H., & Chung, T. (2018). Autophagy-related (ATG) 11, ATG9 and the phosphatidylinositol 3-kinase control ATG2-mediated formation of autophagosomes in Arabidopsis. *Plant Cell Reports*, *37*(4), 653–664. https://doi.org/10.1007/s00299-018-2258-9

Kotkar, H., & Giri, A. (2020). Plant epigenetics and the 'intelligent' priming system to combat biotic stress. *Epigenetics of the Immune System*, 25–38. https://doi.org/10.1016/B978-0-12-817964-2.00002-2

550 Li, Z., & Howell, S. H. (2021). Review: The two faces of IRE1 and their role in protecting plants from
551 stress. *Plant Science*, *303*, 110758. https://doi.org/10.1016/J.PLANTSCI.2020.110758
552 Liu, H., Able, A. J., & Able, J. A. (2021). Priming crops for the future : rewiring stress memory. *Trends in*
553 *Plant Science*, *xx*(xx), 1–18. https://doi.org/10.1016/j.tplants.2021.11.015
554 Liu, Y., Burgos, J. S., Deng, Y., Srivastava, R., Howell, S. H., & Bassham, D. C. (2012). Degradation of the
555 endoplasmic reticulum by autophagy during endoplasmic reticulum stress in Arabidopsisc w. *Plant*
556 *Cell*, *24*(11), 4635–4651. https://doi.org/10.1105/tpc.112.101535
557 Lobell, D. B., Sibley, A., & Ivan Ortiz-Monasterio, J. (2012). Extreme heat effects on wheat senescence in
558 India. *Nature Climate Change 2012 2:3*, *2*(3), 186–189. https://doi.org/10.1038/nclimate1356
559 Löchli, K., Torbica, E., Haile-Weldeslasie, M., Baku, D., Aziz, A., Bublak, D., & Fragkostefanakis, S.
560 (2023). Crosstalk between endoplasmic reticulum and cytosolic unfolded protein response in tomato.
561 *Cell Stress and Chaperones*, *28*(5), 511–528. https://doi.org/10.1007/s12192-022-01316-7
562 Long, S. P., & Ort, D. R. (2010). More than taking the heat: crops and global change. *Current Opinion in*
563 *Plant Biology*, *13*(3), 240–247. https://doi.org/10.1016/J.PBI.2010.04.008
564 Maurel, M., Chevet, E., Tavernier, J., & Gerlo, S. (2014). Getting RIDD of RNA: IRE1 in cell fate
565 regulation. *Trends in Biochemical Sciences*, *39*(5), 245–254.
566 https://doi.org/10.1016/J.TIBS.2014.02.008
567 McLoughlin, F., Kim, M., Marshall, R. S., Vierstra, R. D., & Vierling, E. (2019). HSP101 Interacts with the
568 Proteasome and Promotes the Clearance of Ubiquitylated Protein Aggregates. *Plant Physiology*,
569 *180*(4), 1829–1847. https://doi.org/10.1104/PP.19.00263
570 Mesihovic, A., Ullrich, S., Rosenkranz, R. R. E., Gebhardt, P., Bublak, D., Eich, H., Weber, D., Berberich,
571 T., Scharf, K. D., Schleiff, E., & Fragkostefanakis, S. (2022). HsfA7 coordinates the transition from
572 mild to strong heat stress response by controlling the activity of the master regulator HsfA1a in tomato.
573 *Cell Reports*, *38*(2), 110224. https://doi.org/10.1016/J.CELREP.2021.110224
574 Mittler, R., Finka, A., & Goloubinoff, P. (2012). How do plants feel the heat? *Trends in Biochemical*
575 *Sciences*, *37*(3), 118–125. https://doi.org/10.1016/J.TIBS.2011.11.007
576 Mogk, A., Bukau, B., & Kampinga, H. H. (2018). Cellular Handling of Protein Aggregates by
577 Disaggregation Machines. *Molecular Cell*, *69*(2), 214–226.
578 https://doi.org/10.1016/J.MOLCEL.2018.01.004
579 Nagy-Réder, D., Birinyi, Z., Rakszegi, M., Békés, F., & Gell, G. (2022). The effect of abiotic stresses on the
580 protein composition of four hungarian wheat varieties. *Plants*, *11*(1), 1.
581 https://doi.org/10.3390/PLANTS11010001/S1
582 Nair, A. U., Prasad, D., Bhukya, N., Sunkar, R., Chavali, S., Allu, A. D., & Noctor, G. (2022). Molecular
583 basis of priming-induced acquired tolerance to multiple abiotic stresses in plants. *Journal of*
584 *Experimental Botany*, *73*(11), 3355–3371. https://doi.org/10.1093/JXB/ERAC089
585 Nawkar, G. M., Lee, E. S., Shelake, R. M., Park, J. H., Ryu, S. W., Kang, C. H., & Lee, S. Y. (2018).
586 Activation of the transducers of unfolded protein response in plants. *Frontiers in Plant Science*, *9*, 214.
587 https://doi.org/10.3389/FPLS.2018.00214/BIBTEX
588 Nelson, B. K., Cai, X., & Nebenführ, A. (2007). A multicolored set of in vivo organelle markers for co-
589 localization studies in Arabidopsis and other plants. *The Plant Journal*, *51*(6), 1126–1136.
590 https://doi.org/10.1111/J.1365-313X.2007.03212.X
591 Noh, S. W., Seo, R.-R., Park, H. J., & Jung, H. W. (2021). Two Arabidopsis Homologs of Human Lysine-
592 Specific Demethylase Function in Epigenetic Regulation of Plant Defense Responses. *Frontiers in*
593 *Plant Science*, *0*, 1133. https://doi.org/10.3389/FPLS.2021.688003

Ohama, N., Sato, H., Shinozaki, K., & Yamaguchi-Shinozaki, K. (2017). Transcriptional Regulatory Network of Plant Heat Stress Response. In *Trends in Plant Science* (Vol. 22, Issue 1, pp. 53–65). Elsevier Ltd. https://doi.org/10.1016/j.tplants.2016.08.015

Pastor-Cantizano, N., Ko, D. K., Angelos, E., Pu, Y., & Brandizzi, F. (2020). Functional Diversification of ER Stress Responses in Arabidopsis. *Trends in Biochemical Sciences*, *45*(2), 123–136. https://doi.org/10.1016/J.TIBS.2019.10.008

Phukan, U. J., Stael, S., Gonçalves, A., Van Breusegem, F., & Coll, N. S. (2023). Detection and Quantification of Protein Aggregates in Plants. In *Methods in Molecular Biology* (Vol. 2581, pp. 221–228). Humana Press Inc. https://doi.org/10.1007/978-1-0716-2784-6_15

Pu, Y., Luo, X., & Bassham, D. C. (2017). Tor-dependent and -independent pathways regulate autophagy in arabidopsis thaliana. *Frontiers in Plant Science*, *8*, 1204. https://doi.org/10.3389/FPLS.2017.01204/BIBTEX

Pu, Y., Ruberti, C., Angelos, E. R., & Brandizzi, F. (2019). AtIRE1C, an unconventional isoform of the UPR master regulator AtIRE1, is functionally associated with AtIRE1B in Arabidopsis gametogenesis. *Plant Direct*, *3*(11). https://doi.org/10.1002/pld3.187

Raffeiner, M., Zhu, S., González-Fuente, M., & Üstün, S. (2023). Interplay between autophagy and proteasome during protein turnover. *Trends in Plant Science*, *28*(6), 698–714. https://doi.org/10.1016/J.TPLANTS.2023.01.013

Raught, B., Gingras, A. C., & Sonenberg, N. (2001). The target of rapamycin (TOR) proteins. *Proceedings of the National Academy of Sciences of the United States of America*, *98*(13), 7037–7044. https://doi.org/10.1073/PNAS.121145898

Richter, K., Haslbeck, M., & Buchner, J. (2010). The Heat Shock Response: Life on the Verge of Death. *Molecular Cell*, *40*(2), 253–266. https://doi.org/10.1016/J.MOLCEL.2010.10.006/ASSET/54785DAF-4BAF-48EF-9C3C-98716B4FC179/MAIN.ASSETS/GR3.JPG

Rosenzweig, R., Nillegoda, N. B., Mayer, M. P., & Bukau, B. (2019). The Hsp70 chaperone network. *Nature Reviews Molecular Cell Biology 2019 20:11*, *20*(11), 665–680. https://doi.org/10.1038/s41580-019-0133-3

Samantaray, D., Vankanavath, A. B., Kadumuri, R. V., Ramadurai, D., Chavali, S., & Allu, A. D. (2023). Thermopriming mitigates the effects of heat stress by modulating the expression of Heat shock factors in Brassica juncea (Indian mustard). *Environmental and Experimental Botany*, *211*, 105371. https://doi.org/10.1016/J.ENVEXPBOT.2023.105371

Schmitt, J., Offermann, F., Söder, M., Frühauf, C., & Finger, R. (2022). Extreme weather events cause significant crop yield losses at the farm level in German agriculture. *Food Policy*, *112*, 102359. https://doi.org/10.1016/J.FOODPOL.2022.102359

Schneider, C. A., Rasband, W. S., & Eliceiri, K. W. (2012). NIH Image to ImageJ: 25 years of image analysis. In *Nature Methods* (Vol. 9, Issue 7, pp. 671–675). https://doi.org/10.1038/nmeth.2089

Sedaghatmehr, M., Thirumalaikumar, V. P., Kamranfar, I., Marmagne, A., Masclaux-Daubresse, C., & Balazadeh, S. (2019). A regulatory role of autophagy for resetting the memory of heat stress in plants. *Plant, Cell & Environment*, *42*(3), 1054–1064. https://doi.org/10.1111/PCE.13426

Sedaghatmehr, M., Thirumalaikumar, V. P., Kamranfar, I., Schulz, K., Mueller-Roeber, B., Sampathkumar, A., & Balazadeh, S. (2021). Autophagy complements metalloprotease FtsH6 in degrading plastid heat shock protein HSP21 during heat stress recovery. *Journal of Experimental Botany*, *72*(21), 7498–7513. https://doi.org/10.1093/jxb/erab304

Selinski, J., Frings, S., & Schmidt-Schippers, R. (2024). Perception and processing of stress signals by plant mitochondria. *The Plant Journal*, *120*(6), 2337. https://doi.org/10.1111/TPJ.17133

Serrano, N., Ling, Y., Bahieldin, A., & Mahfouz, M. M. (2019). Thermopriming reprograms metabolic homeostasis to confer heat tolerance. *Scientific Reports 2019 9:1*, *9*(1), 1–14. https://doi.org/10.1038/s41598-018-36484-z

Sharma, I., Talakayala, A., Tiwari, M., Asinti, S., & Kirti, P. B. (2024). A synchronized symphony: Intersecting roles of ubiquitin proteasome system and autophagy in cellular degradation. *Plant Physiology and Biochemistry*, *212*, 108700. https://doi.org/10.1016/J.PLAPHY.2024.108700

Shin, K. D., Lee, H. N., & Chung, T. (2014). A revised assay for monitoring autophagic flux in Arabidopsis Thaliana reveals involvement of autophagy-related9 in autophagy. *Molecules and Cells*, *37*(5), 399–405. https://doi.org/10.14348/molcells.2014.0042

Shpilka, T., Weidberg, H., Pietrokovski, S., & Elazar, Z. (2011). Atg8: an autophagy-related ubiquitin-like protein family. *Genome Biology 2011 12:7*, *12*(7), 1–11. https://doi.org/10.1186/GB-2011-12-7-226

Signorelli, S., Tarkowski, Ł. P., Van den Ende, W., & Bassham, D. C. (2019). Linking Autophagy to Abiotic and Biotic Stress Responses. *Trends in Plant Science*, *24*(5), 413–430. https://doi.org/10.1016/J.TPLANTS.2019.02.001

Song, G. C., Choi, H. K., & Ryu, C. M. (2015). Gaseous 3-pentanol primes plant immunity against a bacterial speck pathogen, pseudomonas syringae pv. Tomato via salicylic acid and jasmonic acid-dependent signaling pathways in arabidopsis. *Frontiers in Plant Science*, *6*(OCTOBER), 1–7. https://doi.org/10.3389/fpls.2015.00821

Soto-Burgos, J., & Bassham, D. C. (2017). SnRK1 activates autophagy via the TOR signaling pathway in Arabidopsis thaliana. *PLOS ONE*, *12*(8), e0182591. https://doi.org/10.1371/JOURNAL.PONE.0182591

Su, T., Li, X., Yang, M., Shao, Q., Zhao, Y., Ma, C., & Wang, P. (2020). Autophagy: An Intracellular Degradation Pathway Regulating Plant Survival and Stress Response. *Frontiers in Plant Science*, *11*, 164. https://doi.org/10.3389/FPLS.2020.00164/BIBTEX

Sun, J. L., Li, J. Y., Wang, M. J., Song, Z. T., & Liu, J. X. (2021). Protein Quality Control in Plant Organelles: Current Progress and Future Perspectives. *Molecular Plant*, *14*(1), 95–114. https://doi.org/10.1016/J.MOLP.2020.10.011/ASSET/6AEADDB2-BAD0-424B-915F-7ABEC2E3C31F/MAIN.ASSETS/GR4.JPG

Suttangkakul, A., Li, F., Chung, T., & Vierstra, R. D. (2011). The ATG1/ATG13 protein kinase complex is both a regulator and a target of autophagic recycling in Arabidopsis. *The Plant Cell*, *23*(10), 3761–3779. https://doi.org/10.1105/TPC.111.090993

Thirumalaikumar, V. P., Gorka, M., Schulz, K., Masclaux-Daubresse, C., Sampathkumar, A., Skirycz, A., Vierstra, R. D., & Balazadeh, S. (2020). Selective autophagy regulates heat stress memory in Arabidopsis by NBR1-mediated targeting of HSP90.1 and ROF1. *Autophagy*, *17*(9), 2184–2199. https://doi.org/10.1080/15548627.2020.1820778

Tugizimana, F., Mhlongo, M. I., Piater, L. A., & Dubery, I. A. (2018). Metabolomics in Plant Priming Research: The Way Forward? *International Journal of Molecular Sciences*, *19*(6). https://doi.org/10.3390/IJMS19061759

Turgut-Kara, N., Arikan, B., & Celik, H. (2020). Epigenetic memory and priming in plants. *Genetica 2020 148:2*, *148*(2), 47–54. https://doi.org/10.1007/S10709-020-00093-4

679 Upadhyaya, S., Agrawal, S., Gorakshakar, A., & Rao, B. J. (2020). TOR kinase activity in
680 Chlamydomonas reinhardtii is modulated by cellular metabolic states. *FEBS Letters*, *594*(19), 3122–
681 3141. https://doi.org/10.1002/1873-3468.13888
682 Wang, X., Tan, N. W. K., Chung, F. Y., Yamaguchi, N., Gan, E. S., & Ito, T. (2023). Transcriptional
683 Regulators of Plant Adaptation to Heat Stress. In *International Journal of Molecular Sciences* (Vol. 24,
684 Issue 17). Multidisciplinary Digital Publishing Institute (MDPI).
685 https://doi.org/10.3390/ijms241713297
686 Wang, Y., Cai, S., Yin, L., Shi, K., Xia, X., Zhou, Y., Yu, J., & Zhou, J. (2015). Tomato HsfA1a plays a
687 critical role in plant drought tolerance by activating ATG genes and inducing autophagy. *Autophagy*,
688 *11*(11), 2033–2047. https://doi.org/10.1080/15548627.2015.1098798
689 Westman, S. M., Kloth, K. J., Hanson, J., Ohlsson, A. B., & Albrectsen, B. R. (2019). Defence priming in
690 Arabidopsis – a Meta-Analysis. *Scientific Reports 2019 9:1*, *9*(1), 1–13.
691 https://doi.org/10.1038/s41598-019-49811-9
692 Wilkinson, S. W., Mageroslashy, M. H., Lopez Sanchez, A., Smith, L. M., Furci, L., Cotton, T. E. A.,
693 Krokene, P., & Ton, J. (2019). Surviving in a Hostile World: Plant Strategies to Resist Pests and
694 Diseases. *Https://Doi.Org/10.1146/Annurev-Phyto-082718-095959*, *57*, 505–529.
695 https://doi.org/10.1146/ANNUREV-PHYTO-082718-095959
696 Xie, D. L., Huang, H. M., Zhou, C. Y., Liu, C. X., Kanwar, M. K., Qi, Z. Y., & Zhou, J. (2022). HsfA1a
697 confers pollen thermotolerance through upregulating antioxidant capacity, protein repair, and
698 degradation in Solanum lycopersicum L. *Horticulture Research*, *9*. https://doi.org/10.1093/hr/uhac163
699 Yamamoto, T., Hoshikawa, K., Ezura, K., Okazawa, R., Fujita, S., Takaoka, M., Mason, H. S., Ezura, H., &
700 Miura, K. (2018). Improvement of the transient expression system for production of recombinant
701 proteins in plants. *Scientific Reports 2018 8:1*, *8*(1), 1–10. https://doi.org/10.1038/s41598-018-23024-y
702 Yang, C., Li, X., Yang, L., Chen, S., Liao, J., Li, K., Zhou, J., Shen, W., Zhuang, X., Bai, M., Bassham, D.
703 C., & Gao, C. (2023). A positive feedback regulation of SnRK1 signaling by autophagy in plants.
704 *Molecular Plant*. https://doi.org/10.1016/J.MOLP.2023.07.001
705 Yang, X., Srivastava, R., Howell, S. H., & Bassham, D. C. (2016). Activation of autophagy by unfolded
706 proteins during endoplasmic reticulum stress. *Plant Journal*, *85*(1), 83–95.
707 https://doi.org/10.1111/tpj.13091
708 Ye, M., Glauser, G., Lou, Y., Erb, M., & Hu, L. (2019). Molecular Dissection of Early Defense Signaling
709 Underlying Volatile-Mediated Defense Regulation and Herbivore Resistance in Rice. *The Plant Cell*,
710 *31*(3), 687–698. https://doi.org/10.1105/TPC.18.00569
711 Yoo, J. Y., Ko, K. S., Vu, B. N., Lee, Y. E., Choi, H. N., Lee, Y. N., Fanata, W. I. D., Harmoko, R., Lee, S.
712 K., Chung, W. S., Hong, J. C., & Lee, K. O. (2024). IRE1 is implicated in protein synthesis regulation
713 under ER stress conditions in plants. *Plant Physiology and Biochemistry*, *215*, 108963.
714 https://doi.org/10.1016/J.PLAPHY.2024.108963
715 Yoshida, T., Ohama, N., Nakajima, J., Kidokoro, S., Mizoi, J., Nakashima, K., Maruyama, K., Kim, J. M.,
716 Seki, M., Todaka, D., Osakabe, Y., Sakuma, Y., SchöZ, F., Shinozaki, K., & Yamaguchi-Shinozaki, K.
717 (2011). Arabidopsis HsfA1 transcription factors function as the main positive regulators in heat shock-
718 responsive gene expression. *Molecular Genetics and Genomics*, *286*(5–6), 321–332.
719 https://doi.org/10.1007/s00438-011-0647-7
720 Zhou, J., Wang, J., Cheng, Y., Chi, Y. J., Fan, B., Yu, J. Q., & Chen, Z. (2013). NBR1-Mediated Selective
721 Autophagy Targets Insoluble Ubiquitinated Protein Aggregates in Plant Stress Responses. *PLoS*
722 *Genetics*, *9*(1). https://doi.org/10.1371/journal.pgen.1003196

723 Zhou, J., Wang, Z., Wang, X., Li, X., Zhang, Z., Fan, B., Zhu, C., & Chen, Z. (2018). Dicot-specific ATG8-
724 interacting ATI3 proteins interact with conserved UBAC2 proteins and play critical roles in plant stress
725 responses. *Autophagy*, *14*(3), 487–504. https://doi.org/10.1080/15548627.2017.1422856
726 Zhu, S., Estévez, J. M., Liao, H., Zhu, Y., Yang, T., Li, C., Wang, Y., Li, L., Liu, X., Pacheco, J. M., Guo,
727 H., & Yu, F. (2020). The RALF1–FERONIA Complex Phosphorylates eIF4E1 to Promote Protein
728 Synthesis and Polar Root Hair Growth. *Molecular Plant*, *13*(5), 698–716.
729 https://doi.org/10.1016/J.MOLP.2019.12.014
730

731 # Figure Legends

732 **Figure 1: Priming improves survival from severe heat stress.** (A) The experimental paradigm is
733 schematized where 37°C was used as a priming stimulus, followed by recovery at 22°C (optimal growth
734 temperature), and then exposed to 45°C heat-triggering stimulus for indicated time durations. Control
735 (untreated) and unprimed seedlings (subjected to only 45°C) were compared in parallel. (B)
736 Representative seedling images from primed, unprimed and control conditions were monitored over
737 multiple days at 22°C during the stress recovery period. Scale bar, 0.5cm. The growth recovery was
738 quantified based on (C) the number of leaves per plant (n=3 biological replicates, with 16 seedlings per
739 replicate), (D) root length (n=2 biological replicates, with 5 seedlings per replicate), and (E) fresh weight
740 (n=3 biological replicates, with 16 seedlings pooled per replicate) at the indicated time points. Despite an
741 initial growth halt (as observed in root length), primed seedlings resumed growth similar to the control,
742 whereas unprimed plants exhibited complete growth arrest and ultimately failed to survive. Data are
743 presented as mean ± SEM (for leaves per plant) and mean ± SD (for root length and fresh weight).
744 Statistical significance was determined using two-way ANOVA, where the asterisk (** p 0.0036; **** p
745 <0.0001) indicates significant differences between primed and unprimed samples.

746 **Figure 2: Priming leads to an increase in chaperone abundance post-heat stress.** (A) The schematics
747 of the experimental paradigm are represented. 0-3 DPS denote time points where samples were collected
748 (PS-Priming Stimulus, TS-Triggering Stimulus). (B) SDS-PAGE analysis indicates that unprimed
749 seedlings undergo a loss in total protein content by the end of 3 DPS, compared to primed and control
750 (n=2 biological replicates). (C-F) Western blot analysis of HSP17.6, HSP21, HSP70, HSP90, and HSP101
751 proteins for various samples post-heat stress reveals that priming leads to an increase in the abundance of
752 HSPs, which persist even after the removal of stress. In contrast, unprimed seedlings do not show any
753 increase in HSP abundance compared to the control (n=3 biological replicates). α-Tubulin served as a
754 loading control. (G) Expression of *HSP21*, *HSP22*, *HSP70* and *HSP101* reflects fold change compared to
755 control. In the primed, *HSPs* get highly induced upon priming and triggering compared to the control. In
756 contrast, in the unprimed, induced expression for most of the *HSPs* is observed in only 1 DPS. Induced
757 expression of *HSPs* was detected in the primed control (only exposed to 37°C) at after the triggering time
758 point, which subsides with time. The data are presented as mean ± SD (n=3 biological replicates).
759 Statistical significance was calculated using one-way ANOVA (**** p <0.0001; *** p <0.001; ** p
760 <0.01; * p <0.05; ns – not significant).

Figure 3: Priming temporally regulates autophagy and promotes effective aggregate clearance. (A-B) Western blot probing ATG8 revealed that primed seedlings show slightly induced autophagy (as seen by ATG8-PE levels) compared to control at the AP time point, which increased further post-triggering stress (0h to 4h). However, by 1 DPS, autophagy in primed is comparable to control and primed-control levels. In contrast, unprimed seedlings display a surge in the ATG8-PE levels post-stress (0h) that remains higher compared to the control (n=3 biological replicates). Numbers below denote intensity values post-normalisation with respect to corresponding control timepoint. (C-D) Western blot of GFP-ATG8 and free-GFP (both detected using anti-GFP antibody) for various samples at the post-heat stress time points reveals that autophagy flux in unprimed seedlings remain high during the stress recovery period as seen by the high free-GFP levels, whereas autophagy in primed seedlings is similar to control. Line plot represents normalised mean intensity of free-GFP/Total-GFP (GFP-ATG8+free-GFP) at post-heat stress time points (n=2 biological replicates). (E-F) Immunoblot analysis of ubiquitin-conjugated aggregates shows that unprimed seedlings have a higher accumulation of aggregates compared to primed and control seedlings by 1 DPS. Box plot represents normalised mean intensity for ubiquitin, where the dotted line denotes the control value (n=2 biological replicates).

Figure 4: Primed seedlings recover from ER stress while the unprimed seedlings exhibit sustained ER stress. (A-B) *bZIP60* spliced form (*bZIP60s*) was used as a marker to detect ER stress. RT-PCR of *bZIP60s*, *bZIP60u* and *ACT2* for all the conditions at given time points post heat stress suggests that primed seedlings initially experience ER stress but recover by 1 DPS to control levels. However, unprimed seedlings experience sustained ER stress as seen from the presence of high *bZIP60s*. Box plot represents quantification for *bZIP60*(s) / *bZIP60*(s+u(unspliced)), where the dotted line denotes control values (n=2 biological replicates). (C-E) Expression of autophagy inhibitors, *BGLU21*, *PR-14* and *ROSY1* is represented as fold change compared to control across conditions. In primed, expression of autophagy inhibitors was found to be downregulated at AP, BT and AT timepoints, but it comes back to basal levels by 1 DPS. However, in unprimed, autophagy inhibitors are continuously maintained at lower levels post-stress. The data are presented as mean ± SD (n=2 biological replicates). Statistical significance was calculated using one-way ANOVA (**** $p < 0.0001$; *** $p < 0.001$; ** $p < 0.01$; * $p < 0.05$; ns – not significant).

Figure 5: Loss of bZIP60 or IRE1A/B leads to delayed recovery post-priming in response to heat stress. (A) Primary root length measurements indicate a significant difference between *bzip60* primed vs. control, and *ire1a/b* primed vs. control, compared to wild-type primed vs. control at seven days post-stress, indicating a delay in growth recovery in both mutants. Data are presented as median ± SD (n=3 biological replicates, with 6 seedlings per replicate). Statistical significance was calculated using Student's t-test (**** $p < 0.0001$; ns – not significant). (B) Western blot analysis of HSP17.6, HSP21, HSP70, HSP90, and HSP101 proteins for all the conditions across timepoints post-heat stress reveals that priming leads to an increase in the abundance of HSPs in *bzip60* and *ire1a/b* mutants, which persist even after the removal of stress. Unprimed *bzip60* and *ire1a/b* seedlings do not show any increase in HSP levels, similar to unprimed wild-type (n=3 biological replicates). (C) Quantification of immunoblots revealed that HSP17.6 displays a similar pattern of increase in protein levels post-priming, across genotypes, compared

800 to WT. A delay in the maximal induction of other HSPs was observed in the mutants compared to WT.
801 (D) Expression of *HSP21*, *HSP22*, *HSP70* and *HSP101* in *bzip60* and *ire1a/b* lines across all the conditions
802 at indicated time points (AP – After priming, BT - Before triggering, AT - After triggering (Day 0), DPS
803 - Days post-stress). In the primed, *HSPs* get highly induced upon priming and triggering, whereas in the
804 unprimed, induced expression for most of the *HSPs* is observed only by 1 DPS. Heat map represents mean
805 expression values (n=2/3 biological replicates). Statistical significance was calculated using one-way
806 ANOVA (**** p <0.0001; *** p <0.001; ** p <0.01; * p <0.05; ns – not significant).

807 **Figure 6: HSFA1 is essential for priming-mediated heat stress tolerance.** (A) Expression analysis of
808 *HSFA1a*, *HSFA2* and *HSFA3* was performed for WT across all the conditions. *HSFA1a* expression (except
809 AT/1 DPS in unprimed) does not significantly change across time points, whereas *HSFA2* and *HSFA3*
810 expression significantly increases immediately after priming (n=3 biological replicates). Statistical
811 significance was calculated using one-way ANOVA (**** p <0.0001; ** p <0.01; * p <0.05; ns – not
812 significant). (B) Phenotypic images of *hsfa1a/b/d* (referred to as *a/b/d*), Col-0 and Ws-0 at 6 DPS. The
813 impact of priming on heat stress response was lost in the *a/b/d* mutant compared to Col-0/Ws-0. Unprimed
814 *a/b/d* fail to survive, similar to that of Col-0/Ws-0 post-heat stress (n=3 biological replicates). (C)
815 Immunoblotting for ATG8 shows that autophagy remains highly induced in both primed and unprimed
816 *a/b/d* mutants post-heat stress (n=3 biological replicates). Numbers below denote intensity values post-
817 normalisation with respect to corresponding control timepoint. (D) Immunoblot analysis for HSPs
818 revealed that primed-WT displayed an increased abundance post-priming, while primed *a/b/d* failed to
819 display HSP abundance, potentially contributing to their lethality (n=3 biological replicates). These
820 observations suggest that failure to activate protein protective (chaperone) response can lead to persistent
821 induction of autophagy following severe heat stress.

822 **Figure 7: Schema representing priming-induced regulation of proteostasis aiding in mounting**
823 **acquired thermotolerance.** Upon heat stress, thermoprimed Arabidopsis seedlings experience ER stress,
824 which activates the ER membrane protein IRE1. Activated IRE1, through its RIDD activity, degrades
825 autophagy inhibitors (*BGLU21*, *ROSY1*, and *PR-14*), dynamically regulating autophagy induction under
826 stress. Concurrently, heat stress leads to an increase in the abundance of heat shock proteins (HSPs),
827 mediated by HSFA1 activation. These processes - dynamic autophagy and the HSP response - work in a
828 temporally coordinated manner to maintain protein homeostasis, promoting seedling survival.
829 Additionally, other unidentified regulators may potentially influence autophagy during thermopriming. In
830 contrast, unprimed seedlings lack sufficient HSPs, which may result in persistent autophagy to clear
831 misfolded/damaged proteins. However, this prolonged autophagy causes an imbalance in protein
832 homeostasis, and may ultimately lead to lethality in unprimed seedlings. Created with BioRender.com.

833 ## Supplementary Figures

834 **Figure S1: Priming-mediated autophagy response is TOR/SnRK independent.** Immunoblot analysis
835 of pS6K, S6K, and pAMPK for all the conditions at the given time points. (A-D) TOR kinase activity, as
836 measured by pS6K/S6K levels, does not significantly change post-priming and triggering across
837 conditions compared to control during priming/heat stress. Box plot represents normalised mean intensity

838 for pS6K/S6K where the dotted line denotes control value (n=2 biological replicates). (E-H) The
839 pAMPK/α-Tub levels do not significantly change post-priming and triggering across conditions compared
840 to control, indicating that SnRK activity remains similar during priming/heat stress. Box plot represents
841 normalised mean intensity for pAMPK/α-Tub where the dotted line denotes control value (n=2 biological
842 replicates). α-Tubulin served as a loading control. Statistical significance was calculated using one-way
843 ANOVA, where the differences were identified to be not significant. (AP- After Priming, DPS - Days Post
844 Stress, C - Control, P - Primed, UP - Unprimed, PC - Primed Control).

845 **Figure S2: Unprimed seedlings exhibit sustained ER stress.** (A) ER stress was determined by checking
846 the presence of *bZIP60* spliced form (*bZIP60s*). Expression analysis of *bZIP60s* using qPCR suggests that
847 primed seedlings initially experience ER stress but recover by 1 DPS, whereas unprimed seedlings
848 experience sustained ER stress (n=2 biological replicates). (B) Confocal images of ER-GFP displaying
849 the endoplasmic reticulum (ER) in the leaves of seedlings across different conditions. Primed seedlings
850 exhibit GFP signals similar to the control, whereas the loss of GFP in unprimed suggests degradation of
851 the ER. Scale bar, 20μm. (n=16 seedlings were imaged from 4 biologically independent experiments).

852 **Figure S3: Identification and testing of homozygous knockout *bzip60* and *ire1a/b* lines for their**
853 **priming-induced heat stress response.** (A) Samples b1 to b10 represent different *bzip60* mutant lines,
854 WT1/4 represent wild-type, and NTC is no template control. Seeds harvested from samples b7, b8 and
855 b10 identified as homozygous *bzip60* knockout lines were used for the experiments. (B) Samples 1-1 to
856 3-4 represent different *ire1a/b* mutant lines, WT is wild-type, and NTC is no template control. Seeds
857 harvested from samples 1-3, 2-1, 2-2, 2-3 and 2-4 identified as homozygous *ire1a/b* knockout lines were
858 used for the experiments. The *bzip60* and *ire1a/b* homozygous lines were subjected to the priming
859 paradigm. Primed (C) *bzip60* and (D) *ire1a/b* knockout mutants were observed to survive severe heat
860 stress post-priming, whereas unprimed seedlings failed to survive.

861 **Figure S4: Autophagy remains induced in *bzip60* and *ire1a/b* mutants post-heat stress.** Western blot
862 probing for ATG8 in (A) *bzip60* and (B) *ire1a/b* mutants post-heat stress reveals that autophagy is induced
863 post-triggering (0 DPS) in primed seedlings; however, it reverts back to control levels during the stress
864 recovery period (1-3 DPS). However, in unprimed (*bzip60* and *ire1a/b*), autophagy is induced post-
865 triggering stress and stays high even after removal of stress (n=2/3 biological replicates). α-Tubulin served
866 as a loading control.

867 **Figure S5: Unprimed samples may experience protein translational arrest post-heat stress.**
868 Immunoblot analysis shows induced levels of HSP101 in primed (both soluble and insoluble fractions)
869 post-stress compared to control. HSP101 was undetectable in both the fractions of the unprimed seedlings,
870 indicating a possible arrest in protein translation following heat stress (n=2 biological replicates).

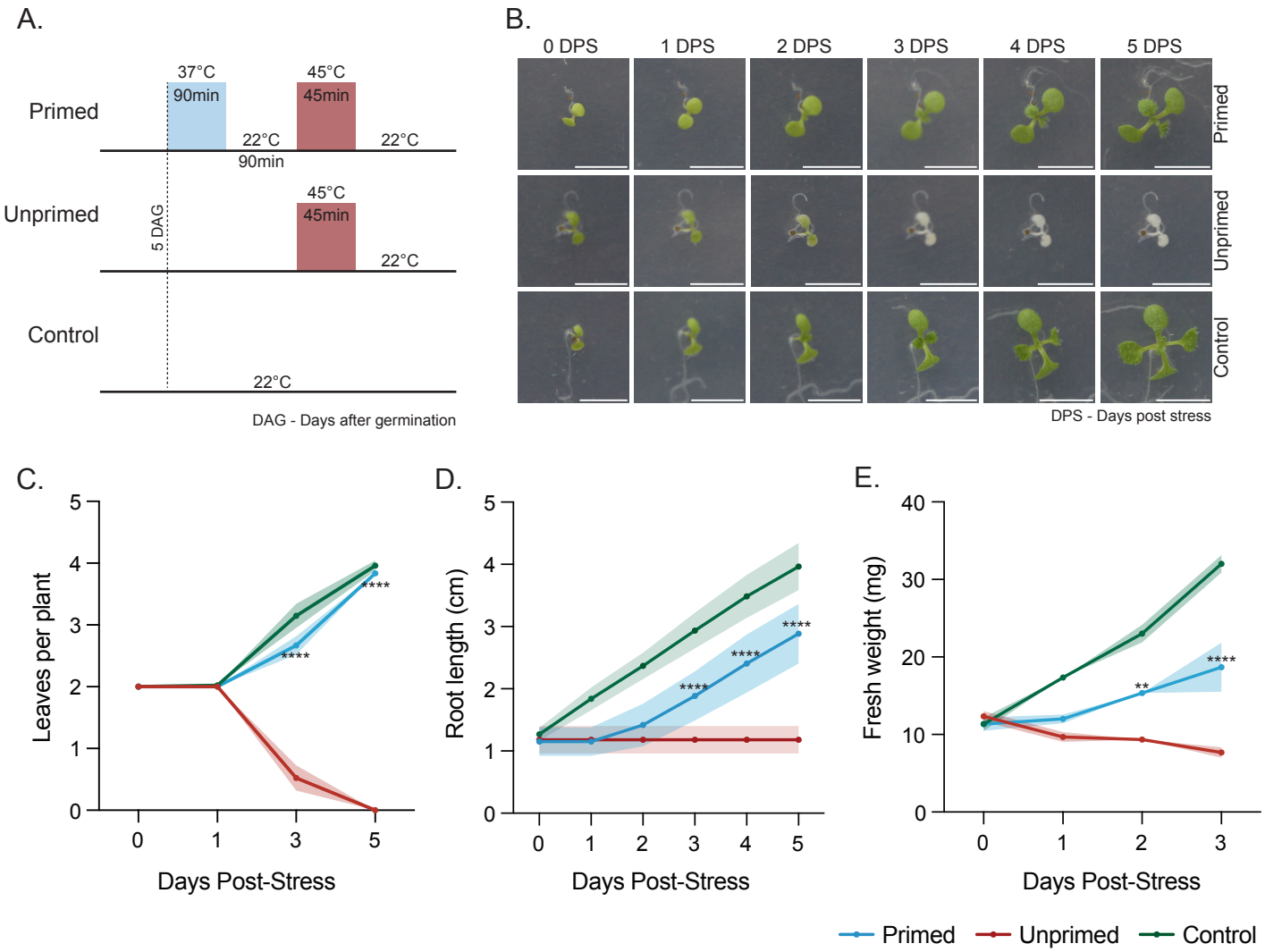

Figure 1: Priming improves survival from severe heat stress. (A) The experimental paradigm is schematised where 37°C was used as a priming stimulus, followed by recovery at 22°C (optimal growth temperature), and then exposed to 45°C heat-triggering stimulus for indicated time durations. Control (untreated) and unprimed seedlings (subjected to only 45°C) were compared in parallel. (B) Representative seedling images from primed, unprimed and control conditions were monitored over multiple days at 22°C during the stress recovery period. Scale bar, 0.5cm. The growth recovery was quantified based on (C) the number of leaves per plant (n=3 biological replicates, with 16 seedlings per replicate), (D) root length (n=2 biological replicates, with 5 seedlings per replicate), and (E) fresh weight (n=3 biological replicates, with 16 seedlings pooled per replicate) at the indicated time points. Despite an initial growth halt (as observed in root length), primed seedlings resumed growth similar to the control, whereas unprimed plants exhibited complete growth arrest and ultimately failed to survive. Data are presented as mean ± SEM (for leaves per plant) and mean ± SD (for root length and fresh weight). Statistical significance was determined using two-way ANOVA, where the asterisk (** p 0.0036; **** p <0.0001) indicates significant differences between primed and unprimed samples.

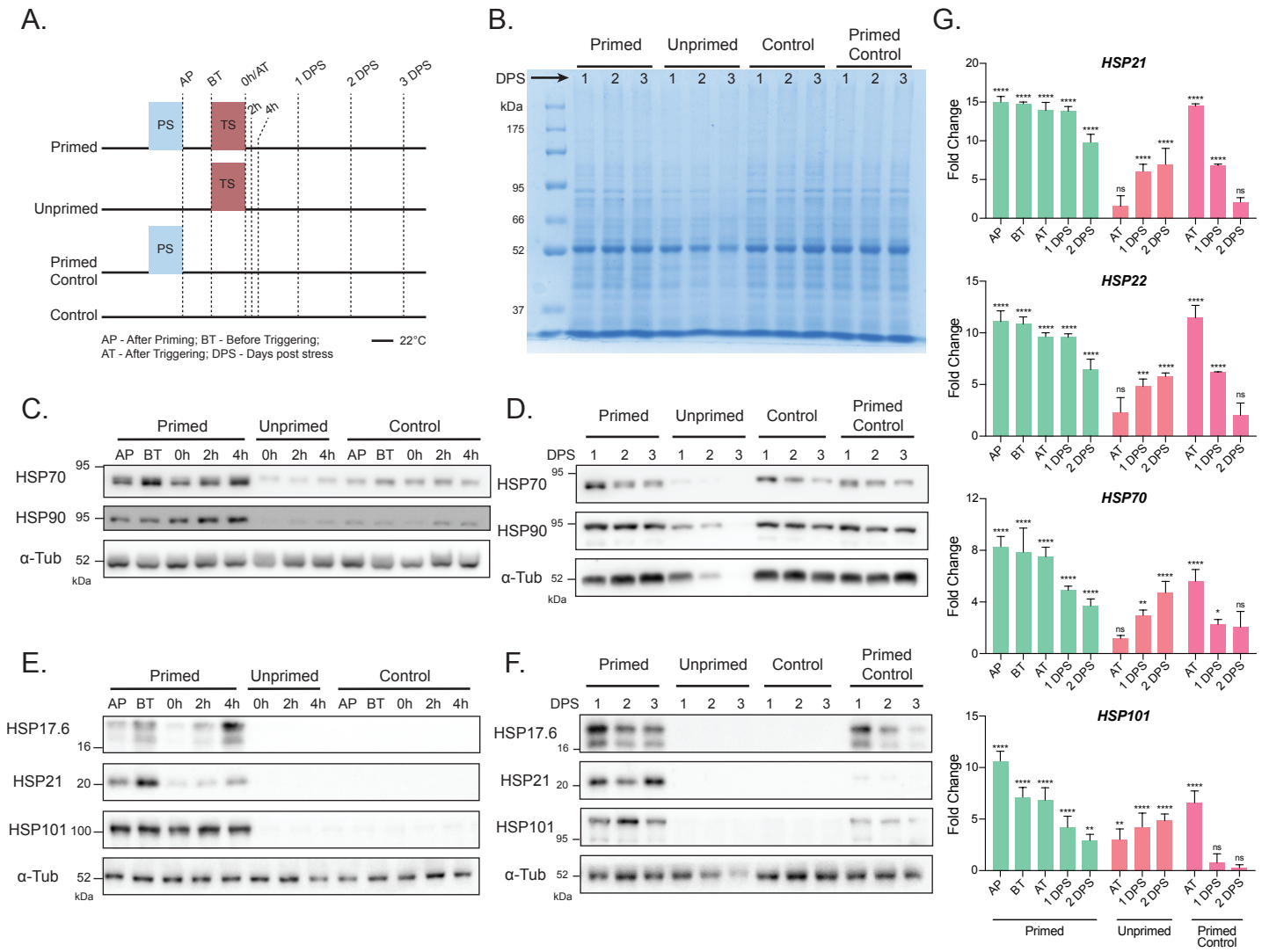

Figure 2: Priming leads to an increase in chaperone abundance post-heat stress. (A) The schematics of the experimental paradigm are represented. 0-3 DPS denote time points where samples were collected (PS-Priming Stimulus, TS-Triggering Stimulus). (B) SDS-PAGE analysis indicates that unprimed seedlings undergo a loss in total protein content by the end of 3 DPS, compared to primed and control (n=2 biological replicates). (C-F) Western blot analysis of HSP17.6, HSP21, HSP70, HSP90, and HSP101 proteins for various samples post-heat stress reveals that priming leads to an increase in the abundance of HSPs, which persist even after the removal of stress. In contrast, unprimed seedlings do not show any increase in HSP abundance compared to the control (n=3 biological replicates). α-Tubulin served as a loading control. (G) Expression of *HSP21*, *HSP22*, *HSP70* and *HSP101* reflects fold change compared to control. In the primed, *HSPs* get highly induced upon priming and triggering compared to the control. In contrast, in the unprimed, induced expression for most of the HSPs is observed in only 1 DPS. Induced expression of *HSPs* was detected in the primed control (only exposed to 37°C) at after the triggering time point, which subsides with time. The data are presented as mean ± SD (n=3 biological replicates). Statistical significance was calculated using one-way ANOVA (**** p <0.0001; *** p <0.001; ** p <0.01; * p <0.05; ns – not significant).

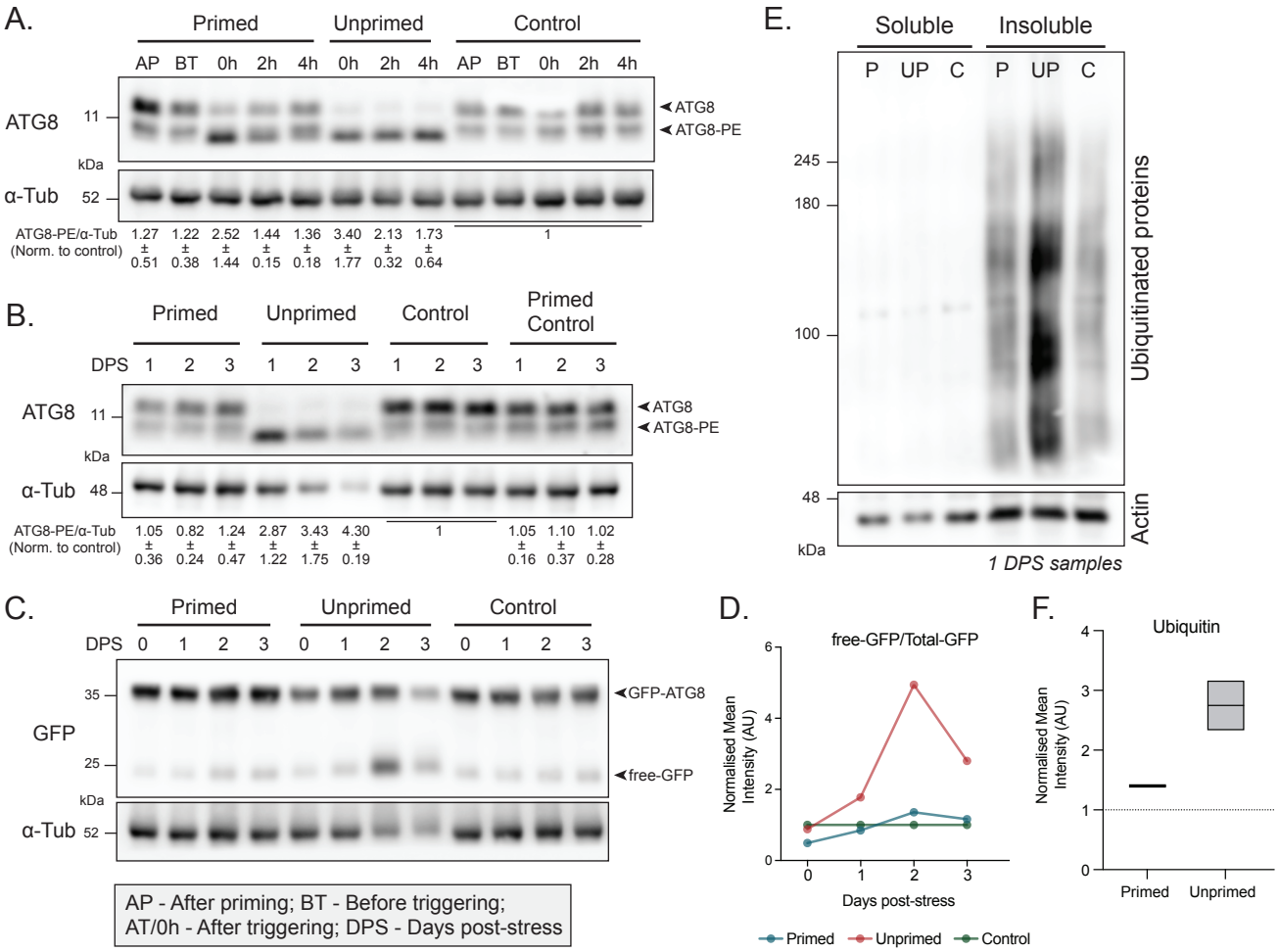

Figure 3: Priming temporally regulates autophagy and promotes effective aggregate clearance. (A-B) Western blot probing ATG8 revealed that primed seedlings show slightly induced autophagy (as seen by ATG8-PE levels) compared to control at the AP time point, which increased further post-triggering stress (0h to 4h). However, by 1 DPS, autophagy in primed is comparable to control and primed-control levels. In contrast, unprimed seedlings display a surge in the ATG8-PE levels post-stress (0h) that remains higher compared to the control (n=3 biological replicates). Numbers below denote intensity values post-normalisation with respect to corresponding control timepoint. (C-D) Western blot of GFP-ATG8 and free-GFP (both detected using anti-GFP antibody) for various samples at the post-heat stress time points reveals that autophagy flux in unprimed seedlings remain high during the stress recovery period as seen by the high free-GFP levels, whereas autophagy in primed seedlings is similar to control. Line plot represents normalised mean intensity of free-GFP/Total-GFP (GFP-ATG8+free-GFP) at post-heat stress time points (n=2 biological replicates). (E-F) Immunoblot analysis of ubiquitin-conjugated aggregates shows that unprimed seedlings have a higher accumulation of aggregates compared to primed and control seedlings by 1 DPS. Box plot represents normalised mean intensity for ubiquitin, where the dotted line denotes the control value (n=2 biological replicates).

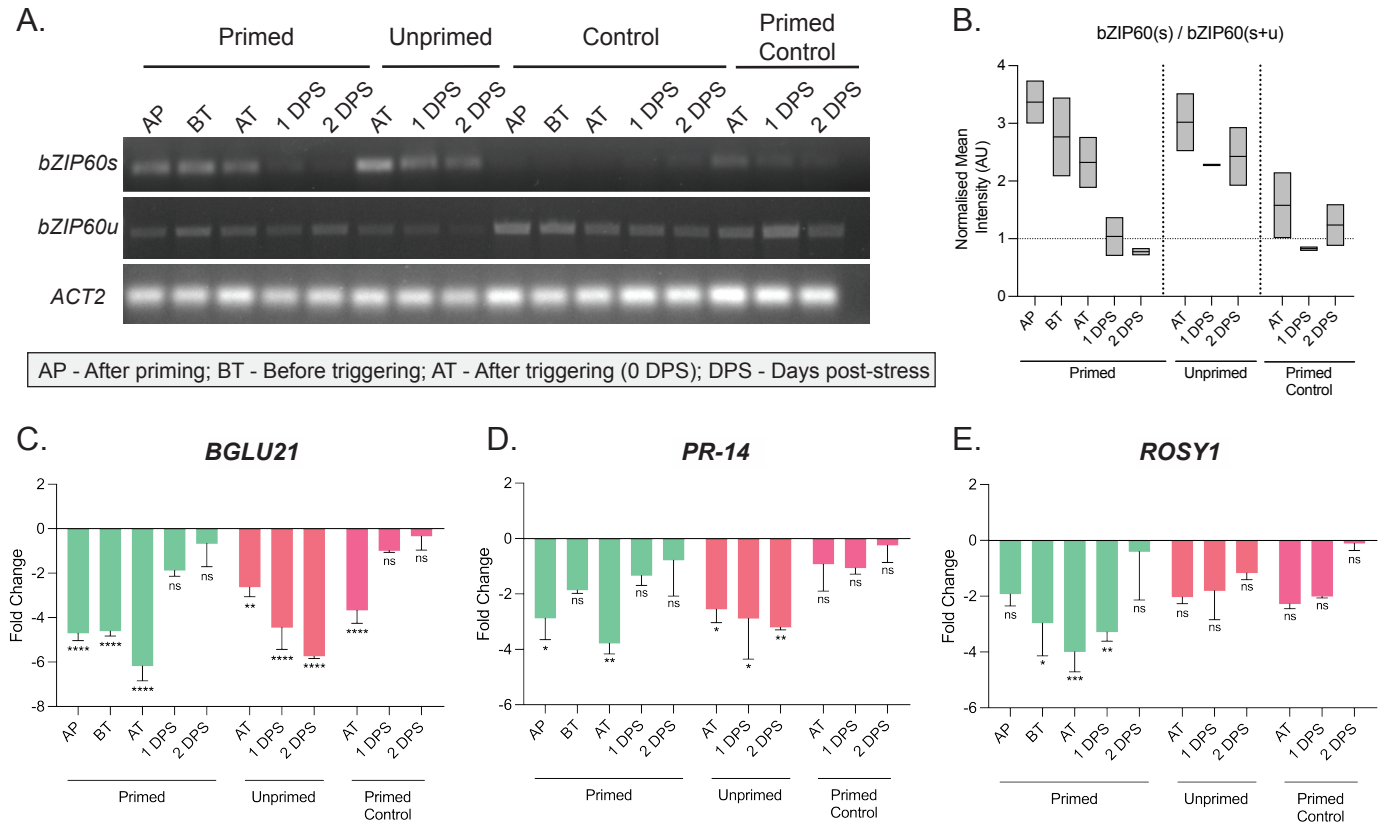

Figure 4: Primed seedlings recover from ER stress while the unprimed seedlings exhibit sustained ER stress. (A-B) *bZIP60* spliced form (*bZIP60s*) was used as a marker to detect ER stress. RT-PCR of *bZIP60s*, *bZIP60u* and *ACT2* for all the conditions at given time points post heat stress suggests that primed seedlings initially experience ER stress but recover by 1 DPS to control levels. However, unprimed seedlings experience sustained ER stress as seen from the presence of high bZIP60s. Box plot represents quantification for *bZIP60*(s) / *bZIP60*(s+u(unspliced)), where the dotted line denotes control values (n=2 biological replicates). (C-E) Expression of autophagy inhibitors, *BGLU21*, *PR-14* and *ROSY1* is represented as fold change compared to control across conditions. In primed, expression of autophagy inhibitors was found to be downregulated at AP, BT and AT timepoints, but it comes back to basal levels by 1 DPS. However, in unprimed, autophagy inhibitors are continuously maintained at lower levels post-stress. The data are presented as mean ± SD (n=2 biological replicates). Statistical significance was calculated using one-way ANOVA (**** p <0.0001; *** p <0.001; ** p <0.01; * p <0.05; ns – not significant).

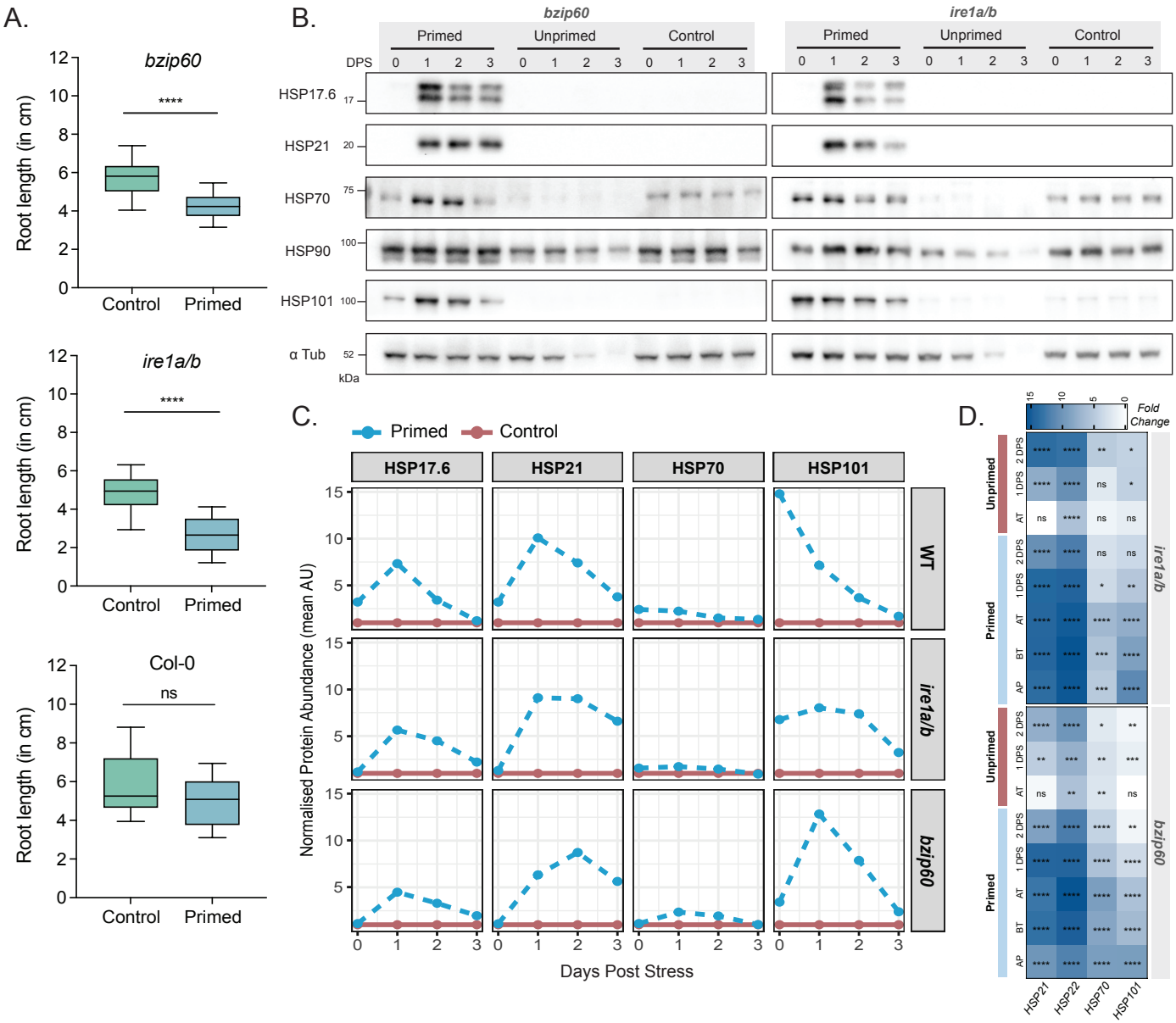

Figure 5: Loss of bZIP60 or IRE1A/B leads to delayed recovery post-priming in response to heat stress. (A) Primary root length measurements indicate a significant difference between *bzip60* primed vs. control, and *ire1a/b* primed vs. control, compared to wild-type primed vs. control at seven days post-stress, indicating a delay in growth recovery in both mutants. Data are presented as median ± SD (n=3 biological replicates, with 6 seedlings per replicate). Statistical significance was calculated using Student's t-test (**** p <0.0001; ns – not significant). (B) Western blot analysis of HSP17.6, HSP21, HSP70, HSP90, and HSP101 proteins for all the conditions across timepoints post-heat stress reveals that priming leads to an increase in the abundance of HSPs in *bzip60* and *ire1a/b* mutants, which persist even after the removal of stress. Unprimed *bzip60* and *ire1a/b* seedlings do not show any increase in HSP levels, similar to unprimed wild-type (n=3 biological replicates). (C) Quantification of immunoblots revealed that HSP17.6 displays a similar pattern of increase in protein levels post-priming, across genotypes, compared to WT. A delay in the maximal induction of other HSPs was observed in the mutants compared to WT. (D) Expression of *HSP21*, *HSP22*, *HSP70* and *HSP101* in *bzip60* and *ire1a/b* lines across all the conditions at indicated time points (AP - After priming, BT - Before triggering, AT - After triggering (Day 0), DPS - Days post-stress). In the primed, *HSPs* get highly induced upon priming and triggering, whereas, in the unprimed, induced expression for most of the *HSPs* is observed only by 1 DPS. Heat map represents mean expression values (n=2/3 biological replicates). Statistical significance was calculated using one-way ANOVA (**** p <0.0001; *** p <0.001; ** p <0.01; * p <0.05; ns – not significant).

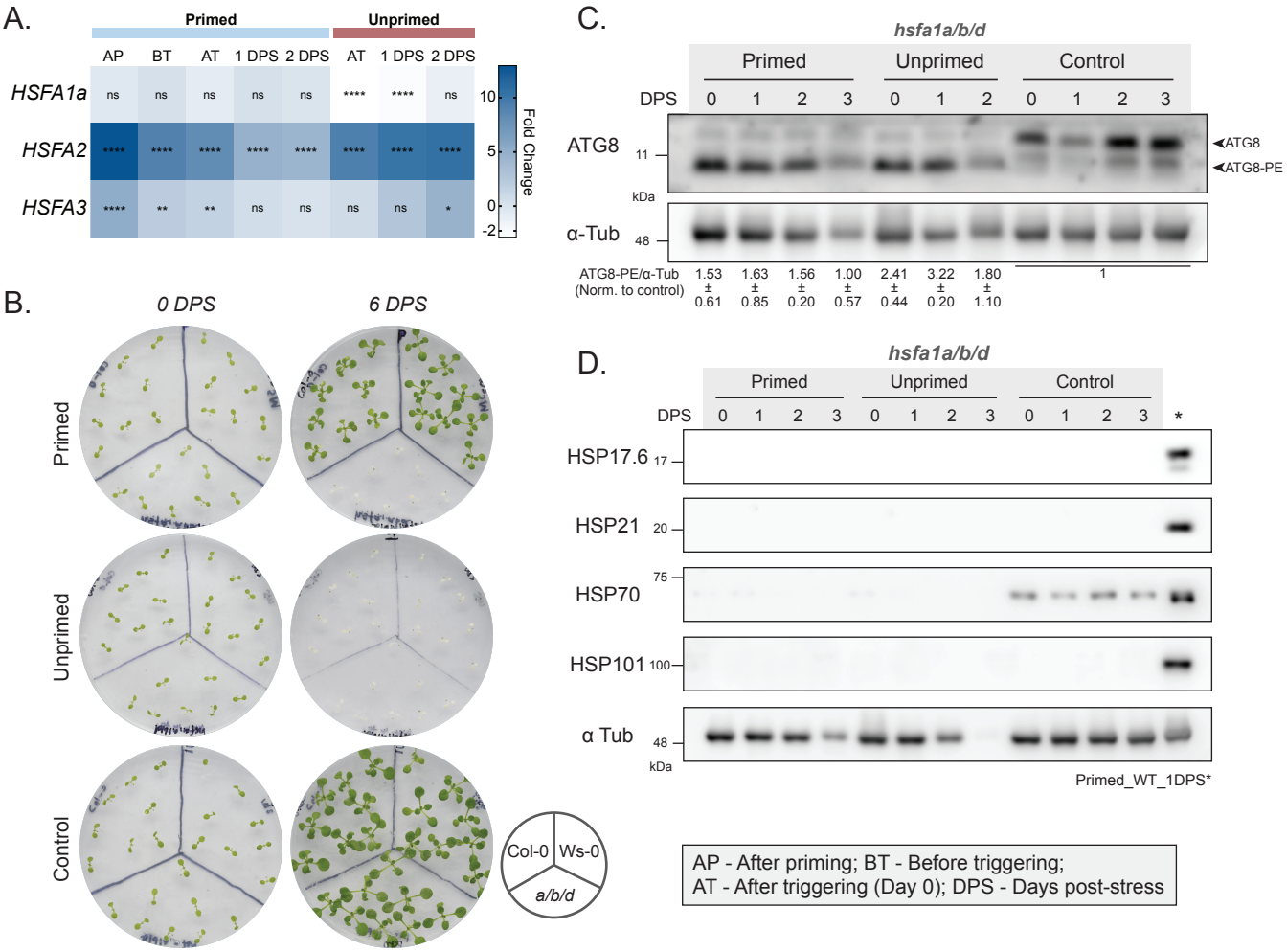

Figure 6: HSFA1 is essential for priming-mediated heat stress tolerance. (A) Expression analysis of *HSFA1a*, *HSFA2* and *HSFA3* was performed for WT across all the conditions. *HSFA1a* expression (except AT/1 DPS in unprimed) does not significantly change across time points, whereas *HSFA2* and *HSFA3* expression significantly increases immediately after priming (n=3 biological replicates). Statistical significance was calculated using one-way ANOVA (**** p <0.0001; ** p <0.01; * p <0.05; ns – not significant). (B) Phenotypic images of *hsfa1a/b/d* (referred to as *a/b/d*), Col-0 and Ws-0 at 6 DPS. The impact of priming on heat stress response was lost in the *a/b/d* mutant compared to Col-0/Ws-0. Unprimed *a/b/d* fail to survive, similar to that of Col-0/Ws-0 post-heat stress (n=3 biological replicates). (C) Immunoblotting for ATG8 shows that autophagy remains highly induced in both primed and unprimed *a/b/d* mutants post-heat stress (n=3 biological replicates). Numbers below denote intensity values post-normalisation with respect to corresponding control timepoint. (D) Immunoblot analysis for HSPs revealed that primed-WT displayed an increased abundance post-priming, while primed *a/b/d* failed to display HSP abundance, potentially contributing to their lethality (n=3 biological replicates). These observations suggest that failure to activate protein protective (chaperone) response can lead to persistent induction of autophagy following severe heat stress.

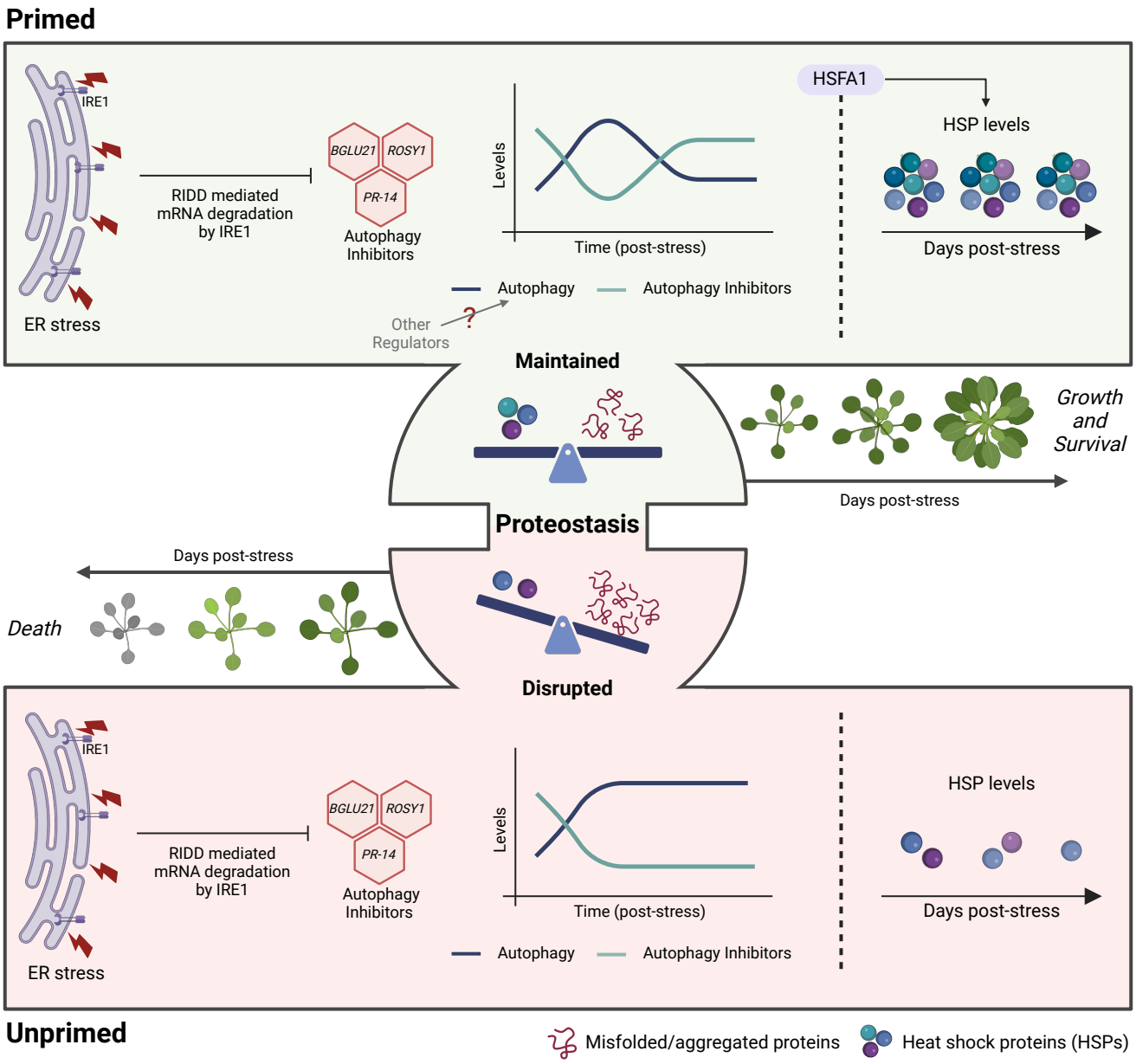

Figure 7: Schema representing priming-induced regulation of proteostasis aiding in mounting acquired thermotolerance. Upon heat stress, thermoprimed *Arabidopsis* seedlings experience ER stress, which activates the ER membrane protein IRE1. Activated IRE1, through its RIDD activity, degrades autophagy inhibitors (*BGLU21*, *ROSY1*, and *PR-14*), dynamically regulating autophagy induction under stress. Concurrently, heat stress leads to an increase in the abundance of heat shock proteins (HSPs), mediated by HSFA1 activation. These processes - dynamic autophagy and the HSP response - work in a temporally coordinated manner to maintain protein homeostasis, promoting seedling survival. Additionally, other unidentified regulators may potentially influence autophagy during thermopriming. In contrast, unprimed seedlings lack sufficient HSPs, which may result in persistent autophagy to clear misfolded/damaged proteins. However, this prolonged autophagy causes an imbalance in protein homeostasis, and may ultimately lead to lethality in unprimed seedlings. Created with BioRender.com.

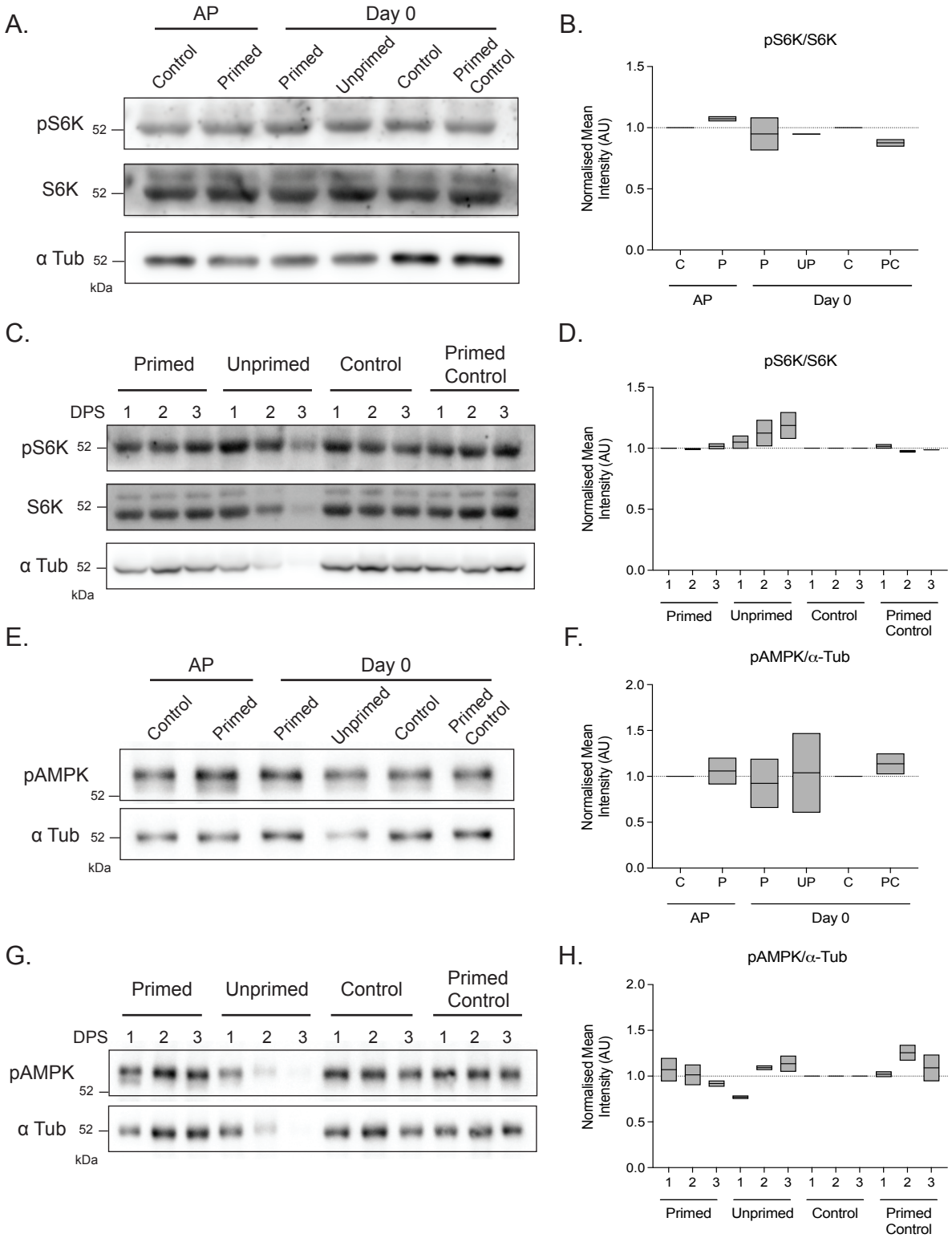

Figure S1: Priming-mediated autophagy response is TOR/SnRK independent. Immunoblot analysis of pS6K, S6K, and pAMPK for all the conditions at the given time points. (A-D) TOR kinase activity, as measured by pS6K/S6K levels, does not significantly change post-priming and triggering across conditions compared to control during priming/heat stress. Box plot represents normalised mean intensity for pS6K/S6K where the dotted line denotes control value (n=2 biological replicates). (E-H) The pAMPK/α-Tub levels do not significantly change post-priming and triggering across conditions compared to control, indicating that SnRK activity remains similar during priming/heat stress. Box plot represents normalised mean intensity for pAMPK/α-Tub where the dotted line denotes control value (n=2 biological replicates). α-Tubulin served as a loading control. Statistical significance was calculated using one-way ANOVA where the differences were identified to be not significant. (AP- After Priming, DPS - Days Post Stress, C - Control, P - Primed, UP - Unprimed, PC - Primed Control).

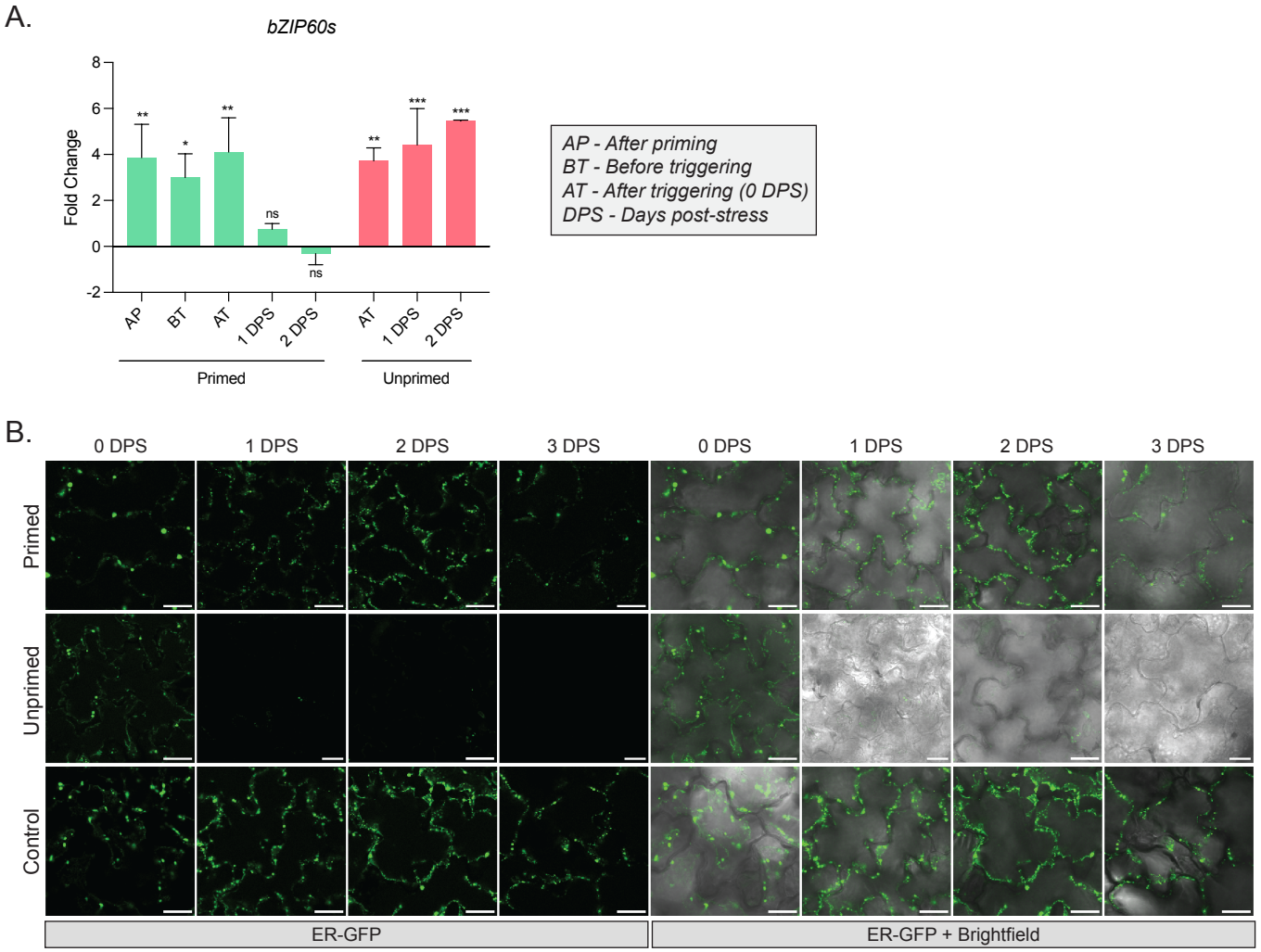

Figure S2: Unprimed seedlings exhibit sustained ER stress. (A) ER stress was determined by checking the presence of *bZIP60* spliced form (*bZIP60s*). Expression analysis of *bZIP60s* using qPCR suggests that primed seedlings initially experience ER stress but recover by 1 DPS, whereas unprimed seedlings experience sustained ER stress (n=2 biological replicates). (B) Confocal images of ER-GFP displaying the endoplasmic reticulum (ER) in the leaves of seedlings across different conditions. Primed seedlings exhibit GFP signals similar to the control, whereas the loss of GFP in unprimed suggests degradation of the ER. Scale bar, 20µm. (n=16 seedlings were imaged from 4 biologically independent experiments).

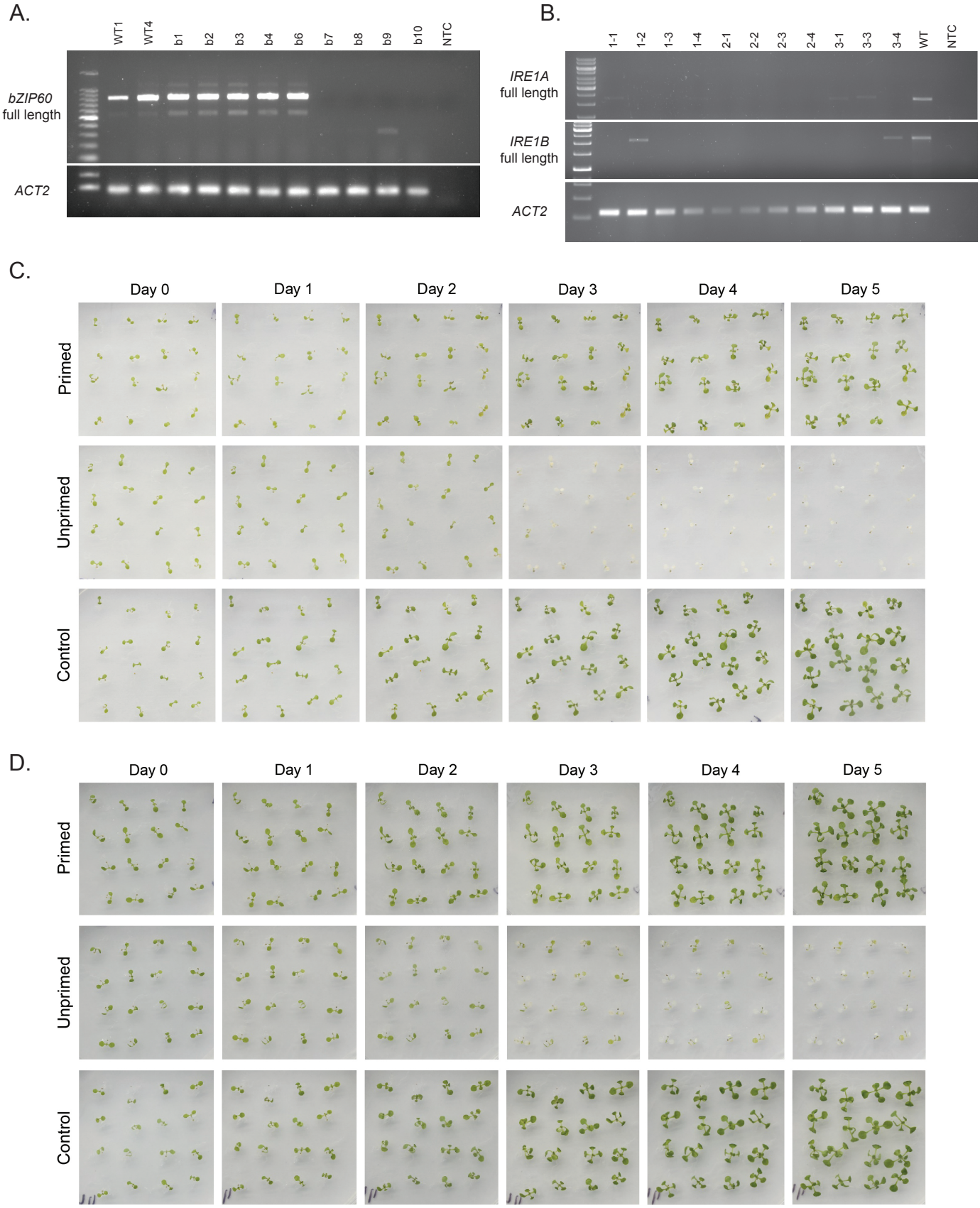

Figure S3: Identification and testing of homozygous knockout *bzip60* and *ire1a/b* lines for their priming-induced heat stress response. (A) Samples b1 to b10 represent different *bzip60* mutant lines, WT1/4 represent wild-type and NTC is no template control. Seeds harvested from samples b7, b8 and b10 identified as homozygous *bzip60* knockout lines were used for the experiments. (B) Samples 1-1 to 3-4 represent different *ire1a/b* mutant lines, WT is wild-type and NTC is no template control. Seeds harvested from samples 1-3, 2-1, 2-2, 2-3 and 2-4 identified as homozygous *ire1a/b* knockout lines were used for the experiments. The *bzip60* and *ire1a/b* homozygous lines were subjected to the priming paradigm. Primed (C) *bzip60* and (D) *ire1a/b* knockout mutants were observed to survive severe heat stress post-priming, whereas unprimed seedlings failed to survive.

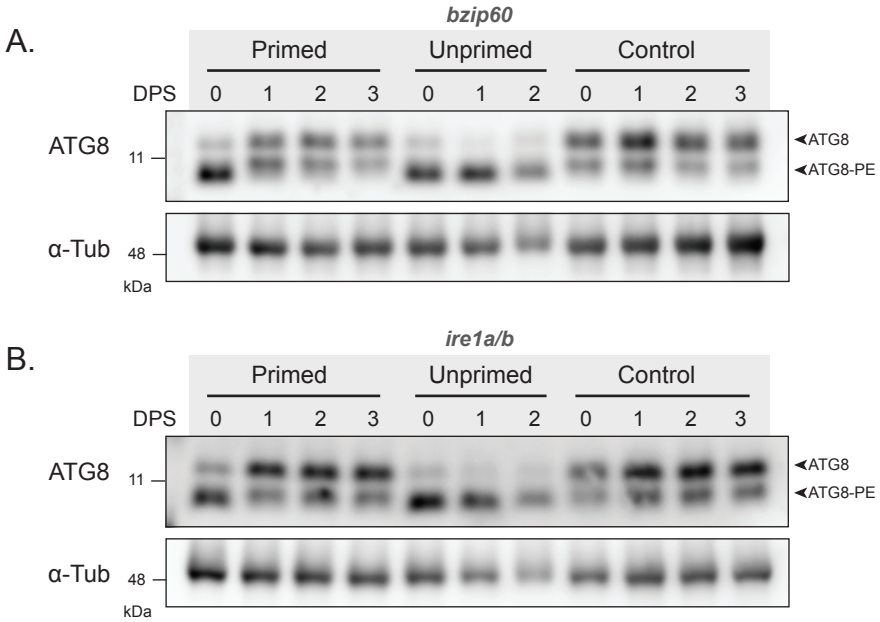

Figure S4: Autophagy remains induced in *bzip60* and *ire1a/b* mutants post-heat stress. Western blot probing for ATG8 in (A) *bzip60* and (B) *ire1a/b* mutants post-heat stress reveals that autophagy is induced post-triggering (0 DPS) in primed seedlings; however, it reverts back to control levels during the stress recovery period (1-3 DPS). However, in unprimed (*bzip60* and *ire1a/b*), autophagy is induced post-triggering stress and stays high even after removal of stress (n=2/3 biological replicates). α-Tubulin served as a loading control.

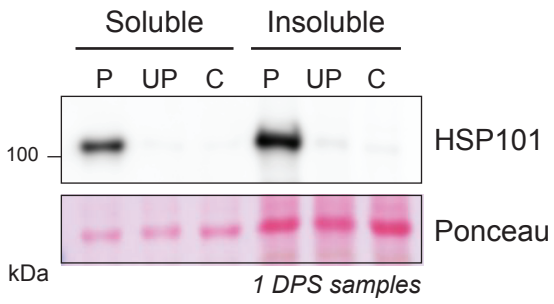

Figure S5: Unprimed samples may experience protein translational arrest post-heat stress. Immunoblot analysis shows induced levels of HSP101 in primed (both soluble and insoluble fractions) post-stress compared to control. HSP101 was undetectable in both the fractions of the unprimed seedlings, indicating a possible arrest in protein translation following heat stress (n=2 biological replicates).